

UNIVERSITY OF PISA
Department of Chemistry and Industrial Chemistry



UNIVERSITÀ DI PISA

In collaboration with

EINDHOVEN UNIVERSITY OF TECHNOLOGY
Department of Chemical Engineering and Chemistry



Master Degree in Chemistry
Curriculum Organic Chemistry

**Synthesis, Characterization and Self-assembly of
Chiral π -Conjugated Systems**

Internal Supervisor: Prof. Lorenzo Di Bari

External Supervisor: Prof. E. W. Meijer

Examiner: Prof. Andrea Pucci

Candidate: Francesco Salerno

Academic Year 2014/2015

“How often people speak of art and science as though they were two entirely different things, with no interconnection. An artist is emotional, they think, and uses only his intuition; he sees all at once and has no need of reason. A scientist is cold, they think, and uses only his reason; he argues carefully step by step, and needs no imagination. That is all wrong. The true artist is quite rational as well as imaginative and knows what he is doing; if he does not, his art suffers. The true scientist is quite imaginative as well as rational, and sometimes leaps to solutions where reason can follow only slowly; if he does not, his science suffers.”

(Isaac Asimov, *The Roving Mind*)

Table of Contents

1	Introduction	1
1.1	Supramolecular Chemistry: “The Chemistry Beyond the Molecule”	1
1.2	Supramolecular Chemistry Basic Principles	3
1.3	Optical and Chiroptical Spectroscopies as Probe for Self-assembly	9
1.4	Naphthalene Diimides: Characteristics and Applications	13
1.5	Chirality in Organic Electronic Devices	19
	Aim of the Thesis	22
2	Results and Discussion	23
2.1	Synthesis and Characterization	23
2.1.1	Amine functionalization of naphthalene tetracarboxylic dianhydride (NTDA)	23
2.1.2	Synthesis of the naphthalene diimides	25
2.2	Thermal and Morphological Properties	28
2.3	Characterization of the N,N'-dialkyl Naphthalene Diimide	30
2.3.1	Optical and chiroptical characterization in solution	30
2.3.2	Solid state characterization	35
2.4	Characterization of the Carboxylic Acid appended Naphthalene Diimide	42
2.4.1	Optical and chiroptical characterization in solution	42
2.4.2	Solid state characterization	49
2.5	Characterization of the Amide Appended Naphthalene Diimide	52
2.5.1	Optical and chiroptical characterization in solution	52
2.5.2	Solid state characterization	54
	Conclusion and Outlook	56
3	Experimental Section	58
3.1	Materials and methods	58
3.2	Synthetic Procedures	60
3.2.1	Synthesis of NMI 1 and NDI 2	60
3.2.2	Synthesis of acid appended NDI 3	61
3.2.3	Synthesis of acid chloride 4	61
3.2.4	Synthesis of amide appended NDI 5	61

Summary

Supramolecular chemistry is the domain of chemistry which exploits non-covalent bonds to obtain self-assembled systems with a bottom-up approach. These assemblies can have opto-electronic properties completely different from the single molecule and their spontaneous formation can be triggered by external parameters like concentration, solvent, pH, etc. In particular, π -conjugated molecules can self-assemble in structures with good semiconducting properties and they can be conveniently employed in organic electronics.

Exploiting chiral non-racemic molecular units, the chirality can be transferred to the supramolecular aggregate. This results in an increase of the preferential absorption and emission of left or right-handed circularly polarized light. So far, these features have allowed the application of these systems in CP-OLED (Circularly Polarized- Organic Light Emitting Diodes), Circularly Polarized detecting OFET (Organic Field Effect Transistors) and Spintronic devices.

In this work, we synthesised and characterized three chiral Naphthalene Diimide (NDI) derivatives, a π -conjugated system, bearing different functional groups: a chiral alkyl chain, a carboxylic acid, and an amide. In suitable conditions, we found that these NDIs could form supramolecular structures with variable chiroptical properties and high anisotropy factors, for application in electronics and spintronics. Thermal and morphological properties of the compound synthesised were assessed via DSC and POM analysis. The self-assembly behaviour, which is strictly related to the opto-electronic properties, was investigated via optical (UV-Vis, PL) and chiroptical (CD, CPL) spectroscopy, in different conditions, both in solution and in solid state.

In the following chapter, an introduction about the supramolecular chemistry and the chiroptical techniques is presented. Furthermore, naphthalene diimide characteristics and some applications of chiral organic molecules in electronic devices are described. The second chapter illustrates the experiments performed to investigate the self-assembly and chiroptical properties of the molecules synthesised. In the third chapter, all the experimental procedures are described.

1 Introduction

1.1 Supramolecular Chemistry: “The Chemistry Beyond the Molecule”

Nature has always inspired researchers about construction of functional dynamic systems through non-covalent interactions. As we know, subtle control on tertiary and quaternary peptides structure is needed to obtain specific properties that could not be possible only through covalent bonds.¹ In plants, photosystem II can funnel efficiently sunlight energy toward reaction centres through precise organization of several chromophores.² An even more famous example is DNA double helix which is kept together by a specific set of hydrogen bonds associated to each nucleotide couple.³

Thus, chemists have tried to imitate nature creating artificial supramolecular systems for several different applications. Intrinsic weakness of most of the intermolecular forces, compared with covalent bonds, could make one think they are not crucial. However, weaker bonds permit formation of bigger structures in reversible and dynamic way which is essential in self-repairing biological architectures. Moreover, the reversibility allows the control of thermodynamically stable structures.⁴

The importance of non-covalent chemistry in the scientific community was amplified when Nobel Prize in chemistry 1987 was awarded jointly to Jean-Marie Lehn, Donald J. Cram and Charles J. Pedersen “for their development and use of molecules with structure-specific interactions of high selectivity”. Lehn defined the supramolecular chemistry as the “chemistry beyond the molecule”.⁵ His work focused on oligo-bipyridines capable of self-assemble in helical structure thanks to anion-metal interactions.^{5,6} He obtained the parallel formation of a double helicate and a triple helicate by self-selection through self-recognition from a mixture of two different type of ligands and metal ions (Figure 1). Cram and Pedersen investigated host-guest interactions in large crown polyethers exploiting high number of ion-dipole forces.^{7,8,9}

¹ Ken A. Dill, *Biochemistry*, **1990**, 29, 7133-7155.

² E. J. Boekema, B. Hankamer, D. Bald, J. Kruip, J. Nield, A. F. Boonstra, J. Barber, M. Rögner, *Proc- Natt Acad Sci USA*, **1995**, 92, 175-179.

³ J. D. Watson, F. H. C. Crick, *Nature*, **1953**, 171, 737-738.

⁴ A. Satake, Y. Kobuke, *Tetrahedron*, **2005**, 61, 13–41.

⁵ J. M. Lehn, *Nobel lecture*, **1987**;

⁶ J. M. Lehn, *Science.*, **2002**, 295, 2400-2403;

⁷ D. J. Cram, J. M. Cram, *Science.*, **1974**, 183 (4127), 803-809;

⁸ D. J. Cram, *Nobel lecture*, **1987**

⁹ C. J. Pedersen, *J. Am. Chem. Soc.*, **1967**, 89 (2495), 7017;

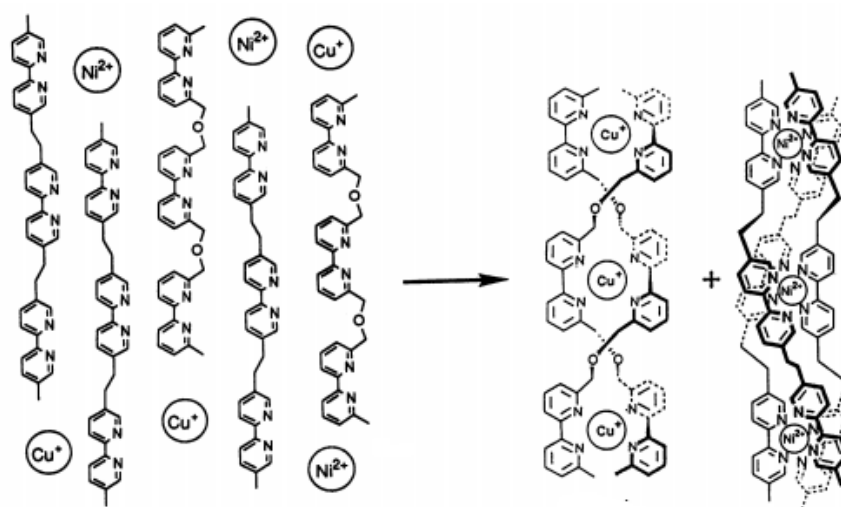


Figure 1. Selective self-assembly of double or triple helicate by self-recognition between two metal cations (Cu^+ , Ni^{2+}) and two oligo-bipyridine ligands¹⁰

Self-assembly is not only a pure academic exercise, but several applications for supramolecular systems so obtained, have just begun to be discovered. Metallic nanowires¹¹, hydrogels for regenerative medicine and drug delivery,¹² fluorescent sensors¹³ and photovoltaic antenna¹⁴ are only some of the applications known so far.

¹⁰ R. Kramer, J.M. Lehn, A. Marquis-Rigault, *Proc. Natl. Acad. Sci. USA*, **1993**, *90*, 5394-5398.

¹¹ V. Faramarzi, F. Niess, E. Moulin, M. Maaloum, J.F. Dayen, J.B. Beaufrand, S. Zanettini, B. Doudin, N. Giuseppone, *Nature Chemistry*, **2012**, *4*, 485-490.

¹² P.Y.W. Dankers, M.J.A. van Luyn, A. Huizinga-van der Vlag, G.M.L. van Gemert, A. H. Petersen, E.W. Meijer, H. M. Janssen, A.W. Bosman, E. R. Popa, *Biomaterials*, **2012**, *33*, 5144-5155.

¹³ X. Ji, Y. Yao, J. Li, X. Yan, F. Huang, *J. Am. Chem. Soc.*, **2013**, *135*, 74-77.

¹⁴ J. Warnan, Y. Pellegrin, E. Blart, F. Odobel, *Chem. Commun.*, **2012**, *48*, 675-677.

1.2 Supramolecular Chemistry Basic Principles

Supramolecular structures are usually obtained by self-recognition of small components which spontaneously (or triggered by environment) self-assemble in more complex systems. This approach, so called bottom-up, is nowadays quite common in designing new experiments. The desired supramolecular architecture can be obtained employing several kind of different interactions: hydrophobic and hydrophilic forces, hydrogen bonding, aromatic π - π stacking, ionic and dipole interactions. Since all of these interactions have different strength and directionality, advantages of each one can be selectively exploited. The most important non-covalent interactions can be summarized as in Table 1.

Table 1. Most important non-covalent interactions and typical strength range¹⁵

Interaction	Strength (kJ mol ⁻¹)	Example
Ion-Ion	200-300	NH ₄ Cl
Ion-dipole	50-200	Sodium [15] crown-5
Dipole-dipole	5-50	Acetone
Hydrogen bonding	4-120	Carboxylic acid, primary and secondary amide, alcohol, amine
Cation- π	5-80	K ⁺ in benzene
π - π	0-50	Benzene and graphite
Van der Waals	< 5 kJ mol ⁻¹ but variable depending on surface area	Argon, packing in molecular crystals
Hydrophobic	Related to solvent-solvent interaction energy	Cyclodextrin inclusion compounds

We will mainly focus on π - π stacking interaction and hydrogen bonding, which can efficiently cooperate together in aromatic carboxylic acids, amides, and other common compounds like those synthesised in this work.^{17,18,19}

¹⁵ J. W. Steed, D. R. Turner, K. J. Wallace, *Core Concepts in Supramolecular Chemistry and Nanochemistry*, John Wiley & Sons, Ltd, **2007**

¹⁷ M. Seo, J. Park, S. Y. Kim, *Org. Biomol. Chem.*, **2012**, *10*, 5332-5342.

¹⁸ T. Mes, S. Cantekin, D. W. R. Balkenende, M. M. M. Frissen, M. A. J. Gillissen, B. F. M. De Waal, I. K. Voets, E. W. Meijer, A. R. A. Palmans.

¹⁹ M. Lackinger, W. M. Heckl, *Langmuir*, **2009**, *25*, 11307–11321.

Hydrogen bonding

Hydrogen bonding is an interaction between a partial positive charge on hydrogen and another electronegative atom with available non-bonding electron lone pairs. The unit bearing the hydrogen atom involved is called donor (D) and the unit bearing the available lone pair is called acceptor (A). Typical good donors and acceptors at the same time are the secondary amides which are well-known to be responsible for peptides secondary and tertiary structure. The carbonyl group of the amide can act as a donor, and the N-H unit can act as an acceptor. Secondary amides. Properties of hydrogen bonding differ greatly from the rest of non-covalent interactions because of their high strength and directionality. As reported in Table 1, their strength can vary in a broad range depending on their number and organization. Array structures are typical supramolecular structures where the importance of a rational molecule design is well visible. In Figure 2, two different arrays are shown. Has been demonstrated that complexes ADA-DAD type show lower dimerization constants compared with AAA-DDD type.²⁰ Reason of this difference seems to lie in repulsive cross interactions between donor or acceptor on different partners, which tend to stabilize the AAA-DDD combination.

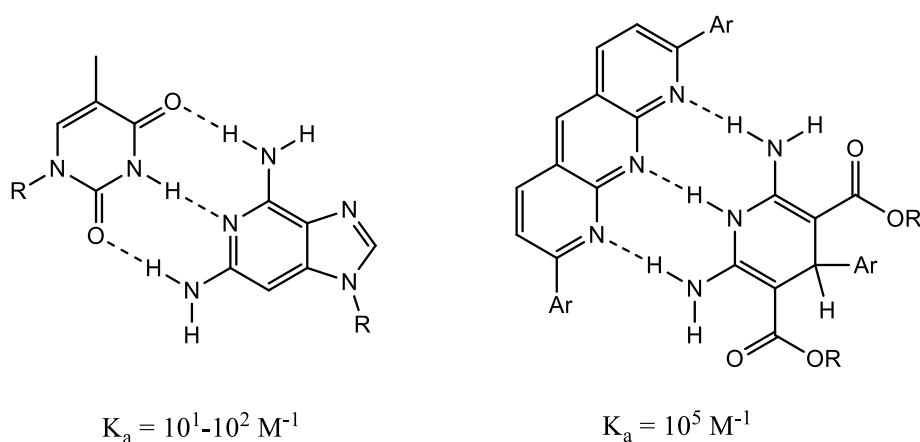


Figure 2. Different H-bonding arrays and association constants. ADA-DAD (left), AAA-DDD (right).

Not only definite stoichiometry complexes, but also supramolecular polymers can be obtained exploiting hydrogen bonding. A typical system which aggregates in one-dimensional columnar stacks is benzene-1,3,5-tricarboxamide (BTA)²¹ shown in Figure 3. Fibers of various diameter can be obtained depending on concentration, temperature and solvent. Generally N-alkyl benzamides show coplanar conformation between the aromatic π -system and the π -orbitals of the amide group, to allow

²⁰ T. J. Murray, S. C. Zimmerman, *J. Am. Chem. Soc.*, **1992**, *114*, 4010-4011.

²¹ S. Cantekin, T. F. A. de Greef, A. R. A. Palmans, *Chem. Soc. Rev.*, **2012**, *41*, 6125-6137.

an optimal overlap. However planarity may be lost during aggregation process. The energy loss due to decreasing of π -conjugation in each molecule is balanced by the formation of three new H-bonds for each BTA unit (Figure 3). Moreover, H-bonding network induces a helical arrangement of the aggregate²² where the preferred handedness can be controlled by chiral non-racemic groups connected to the amide moieties.²³

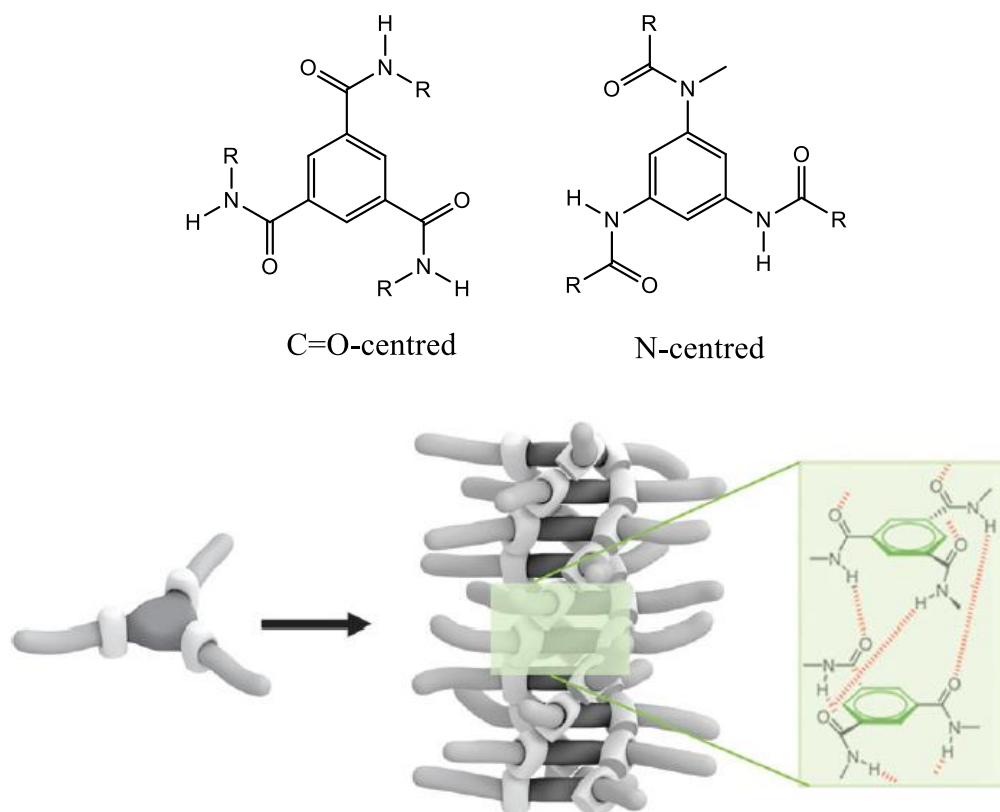


Figure 3. General structures of C=O- and N-centred benzene 1,3,5-tricarboxamides (top). Representation of BTAs columnar stacks and inset of H-bonding connection (bottom).²¹

So far, BTAs fibers networks have been used to obtain hydrogels,²⁴ liquid crystals,²⁵ MRI contrast agents,²⁶ nucleating agents,²⁷ drug delivery systems²⁸ and other applications.

²² M. P. Lightfoot, F. S. Mair, R. G. Pritchard, J. E. Warren, *Chem. Commun.*, **1999**, 1945–1946

²³ L. Brunsveld, A. P. H. J. Schenning, M. A. C. Broeren, H. M. Janssen, J. A. J. M. Vekemans, E. W. Meijer, *Chem. Lett.*, **2000**, 292–293.

²⁴ A. Bernet, R. Q. Albuquerque, M. Behr, S. T. Hoffmann, H.-W. Schmidt, *Soft Matter*, **2012**, *8*, 66–69.

²⁵ Y. Matsunaga, N. Miyajima, Y. Nakayasu, S. Sakai and, M. Yonenaga, *Bull. Chem. Soc. Jpn.*, **1988**, *61*, 207–210.

²⁶ P. Besenius, J. L. M. Heynens, R. Straathof, M. M. L. Nieuwenhuizen, P. H. H. Bomans, E. Terreno, S. Aime, G. J. Strijkers, K. Nicolay, E. W. Meijer, *Contrast Media Mol. Imaging*, **2012**, *7*, 356–361.

²⁷ M. Blomenhofer, S. Ganzleben, D. Hanft, H.-W. Schmidt, M. Kristiansen, P. Smith, K. Stoll, D. Maeder, K. Hoffmann, *Macromolecules*, **2005**, *38*, 3688–3695.

²⁸ K. E. Broaders, S. J. Pastine, S. Grandhe, J. M. J. Frechet, *Chem. Commun.*, **2011**, *47*, 665–667.

π - π Interactions

π -stacking is a type of dipole-induced interaction between π -electron clouds, which commonly arise in aromatic molecules. Stacking of porphyrins,⁴ phthalocyanines,²⁹ oligothiophenes,³⁰ and many others π -conjugated aromatic systems³¹ have been investigated so far. Simple benzene molecules have been found not to adopt facial stacking (so called Sandwich), because of the repulsion between π -electron clouds. On the contrary, interactions of the aromatic core with a C-H bond in a T-shaped or displaced geometry are preferred (Figure 4). However, with the increase in the conjugation of the aromatic system, attractive facial interactions result much more effective. In wider π -electron clouds, induced dipoles can be formed more easily, allowing stronger interactions between aromatic planes. For example, hexabenzocoronenes, a highly conjugated aromatic system, can assemble in nanotubes mainly driven by π - π stacking interactions.³²

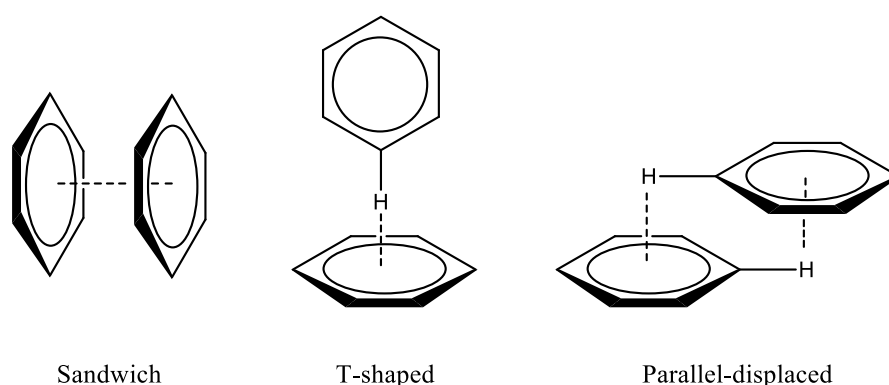


Figure 4. Possible interaction of aromatic electron cloud with another aromatic cloud (sandwich or stacked) or with C-H bond (T-shaped and parallel-displaced). Sandwich structure is not preferred in simple benzene ring due to repulsion between π -electrons.

Strong interactions between extended aromatic molecules are required to have conductive materials. π -conjugated molecules are therefore basic building blocks in organic electronic devices.³¹

One-dimensional aggregation mechanisms

²⁹ P. Weber, D. Guillon, A. Skoulios, *Liquid Crystals*, **1991**, *9*, 369-382.

³⁰ P. Leclère, M. Surin, P. Viville, R. Lazzaroni, A. F. M. Kilbinger, O. Henze, W. J. Feast, M. Cavallini, F. Biscarini, A. P. H. J. Schenning, E. W. Meijer, *Chem. Mater.*, **2004**, *16*, 4452-4466.

³¹ F. J. M. Hoeben, P. Jonkheijm, E. W. Meijer, A. P. H. J. Schenning, *Chem. Rev.* **2005**, *105*, 1491-1546.

³² J. P. Hill, W. Jin, A. Kosaka, T. Fukushima, H. Ichihara, T. Shimomura, K. Ito, T. Hashizume, N. Ishii, T. Aida, *Science*, **2004**, *304*, 1481-1483

An interesting supramolecular motive is the non-covalent one-dimensional polymerization, in which aggregates grow preferentially in a single direction. Several different architectures can be formed in this way, namely fibrils, ribbons, helices and nanotubes.³³ The first supramolecular polymer was synthesised by Fouquey et al.³⁴ in 1990, and units were connected to each other by complementary hydrogen bonding array. As for covalent polymers, polymerization mechanism is important to determine polydispersity and consequently properties of the supramolecular structure. Two main classes of mechanism have been identified (Figure 5). In the isodesmic polymerization, association constant between two units does not depend on their lengths. In the cooperative polymerization instead, a nucleation step and elongation one can be recognized. During the nucleation step the aggregate behaves like in the isodesmic model, but when it reaches a certain length, the association constant becomes more favourable. To precisely control dimensions of the aggregate, controlled living polymerization can be obtained with suitable building blocks and conditions.³⁵ Optical spectroscopy is a common tool to identify the polymerization mechanism. Following the absorption or circular dichroism signal, in function of temperature or concentration, the mechanism can be recognized. Plotting the signal detected by this techniques versus concentration or temperature, the curve shape indicate the mechanism followed.

Isodesmic mechanism is characterized by a sigmoidal curve, while nucleation-elongation exhibits a non-sigmoidal curve as shown in Figure 5.

³³ Y. Yan, Y. Lin, Y. Qiao, J. Huang, *Soft Matter*, **2011**, 7, 6385-6398.

³⁴ C. Fouquey, J.-M. Lehn, A.-M. Levelut, *Adv. Mater.* **2**, **1990**, 254-257.

³⁵ S. Ogi, K. Sugiyasu, S. Manna, S. Samitsu, M. Takeuchi, *Nature Chemistry*, **2014**, 6, 188–195.

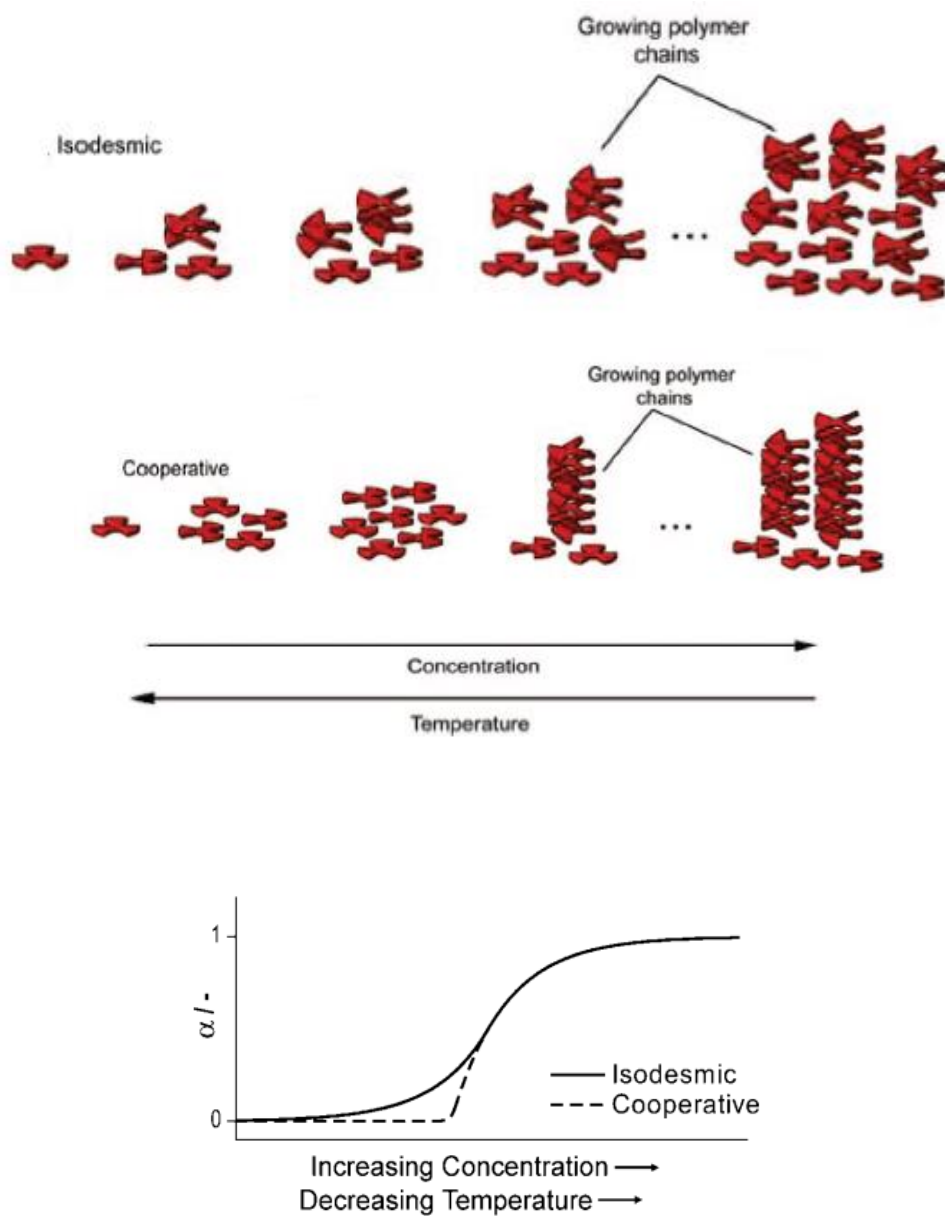


Figure 5. Graphic representation of supramolecular polymerization via isodesmic and cooperative mechanisms (top).³⁶ Simplified representation of the degree of polymerization versus temperature and concentration (bottom).³⁷

³⁶ T. F. A. De Greef, M. M. J. Smulders, M. Wolffs, A. P. H. J. Schenning, R. P. Sijbesma, E. W. Meijer, *Chem. Rev.*, **2009**, *109*, 5687–5754.

³⁷ M. M. J. Smulders, M. M. L. Nieuwenhuizen, T. F. A. de Greef, P. van der Schoot, A. P. H. J. Schenning, E. W. Meijer, *Chem. Eur. J.*, **2010**, *16*, 362 – 367.

1.3 Optical and Chiroptical Spectroscopies as Probe for Self-assembly

Two chromophores with similar transition dipole energies, not conjugated to each other and close in space, interact through dipole-dipole interactions. This interaction has great influence on the spectroscopic properties of the chromophore, which cannot be considered as ‘isolated’ anymore.

As already explained, supramolecular chemistry is characterized by reversible interactions and fast equilibria on molecular scale. Therefore, optical spectroscopies (which are ‘fast’ spectroscopies), have been extensively used to detect changes in electronic properties of molecules undergoing aggregation. When two π -conjugated systems are likely to form a dimer (or oligomer), spectroscopic changes strongly depend of distance and orientation between the chromophores. As consequence of the coupling between two equal chromophores, the two degenerate excited states split into two new levels. According to Kasha’s exciton model,³⁸ two limiting cases can be recognized: H-aggregate, when the chromophores are arranged one on the top of each other, and J-aggregate when a displacement along the transition dipole direction occurs (Figure 6).

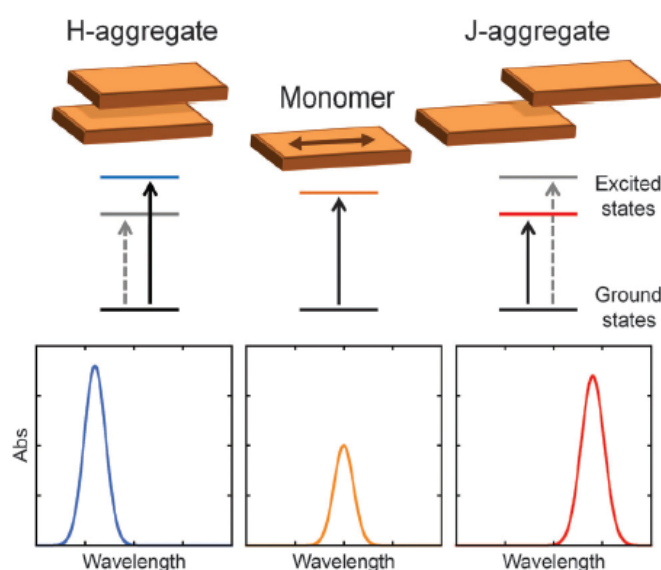


Figure 6. Simple model to rationalise UV-Vis spectral changes when two π -conjugated molecules interact. Solid arrows indicated allowed transitions and dashed arrows forbidden ones.³⁹

In the UV-Vis spectrum, blue-shift is theoretically predicted in the former case, as the transition allowed is at higher energy compared with the monomer. Red-shift instead is predicted for the latter,

³⁸ M. Kasha, H. R. Rawls, M. A. El-Bayoumi, *Pure Appl. Chem.*, **1965**, *11*, 371-392.

³⁹ G. Pescitelli, L. Di Bari, N. Berova, *Chem. Soc. Rev.*, **2014**, *43*, 5211-5233.

as the allowed excited state is at lower energy. H is the initial of Hypsochromic, while J refers to Jelly, who first observed bathochromic shift on cyanine aggregation.⁴⁰

Other characteristics predictable by this simple model are the enhanced fluorescence and small Stokes shift in J-aggregates. Respectively, fluorescence is weakened and Stokes shift is large in H-aggregates. These effects are due to relaxation processes which led the electronic excited molecules to the lowest vibrational state which is superradiant for J-aggregate (almost no energy is lost in relaxation) and non-radiant for H-aggregates. However, most frequent are intermediate cases, where chromophores are arranged in geometries which differ in displacement angle and orientation from limiting cases described above.

For a chiral arrangement of the chromophores, Circular Dichroism (CD) spectroscopy, is a fast technique and results very sensitive to stereochemical issues.⁴¹ Moreover, it is particularly suited to study supramolecular complexes and aggregates. A particular case is represented by molecules containing an extended conjugated moiety (which is usually achiral) and some chiral pendant. Here, the direct action of the dissymmetric environment onto the chromophore may be too weak to give rise to noticeable CD spectra features. The formation of intermolecular aggregates, following the principles sketched above, i.e. possibly π - π attractive interaction between the conjugated groups, combined either with H-bond or steric interaction on the chiral pendant, gives rise to chiral supramolecular structures. In this aggregated form, two or more chromophores are nearby and arranged in dissymmetric form, thus becoming responsible for very prominent CD features, due to degenerate exciton coupling. Since isolated monomers do not interact with each other, they do not contribute to signal in a CD spectrum. Therefore Circular Dichroism provide another sensitive technique to probe aggregation, in solution and solid state as well. Moreover, further information regarding handedness of the aggregate can be obtained, that no other spectroscopies can provide. In a simplified case, an aggregate of rod-like molecules can describe supramolecular helicity, and display a CD signal. Since only the closest neighbour molecules can interact with non-negligible strength, CD spectrum will be given by the sum of all separate signals arising from dimers coupling. The result is a characteristic pair of bands of opposite sign, so called exciton couplet.⁴² The sequence of bands signs is diagnostic of the absolute arrangement of the electric dipole transition moments (Figure 7). Each pair of chromophores contribute to the exciton couplet which represent the chirality

⁴⁰ E. E. Jelley, *Nature*, **1936**, 138, 1009–1010.

⁴¹ N. Berova, L. Di Bari, G. Pescitelli, *Chem. Soc. Rev.*, **2007**, 36, 914-931.

⁴² L. Goerigk, H. Kruse, S. Grimme, Theoretical electronic circular dichroism spectroscopy of large organic and supramolecular systems. In: N. Berova, P. L. Polavarapu, K. Nakanishi, R. W. Woody, *Comprehensive Chiroptical Spectroscopy Vol. 1*, Wiley, **2012**, 65-90.

of the transition dipole moments. A positive chirality (that is a right-handed arrangement of the chromophores) will give a positive sign of the longer wavelength CD signal, and viceversa for the negative chirality.

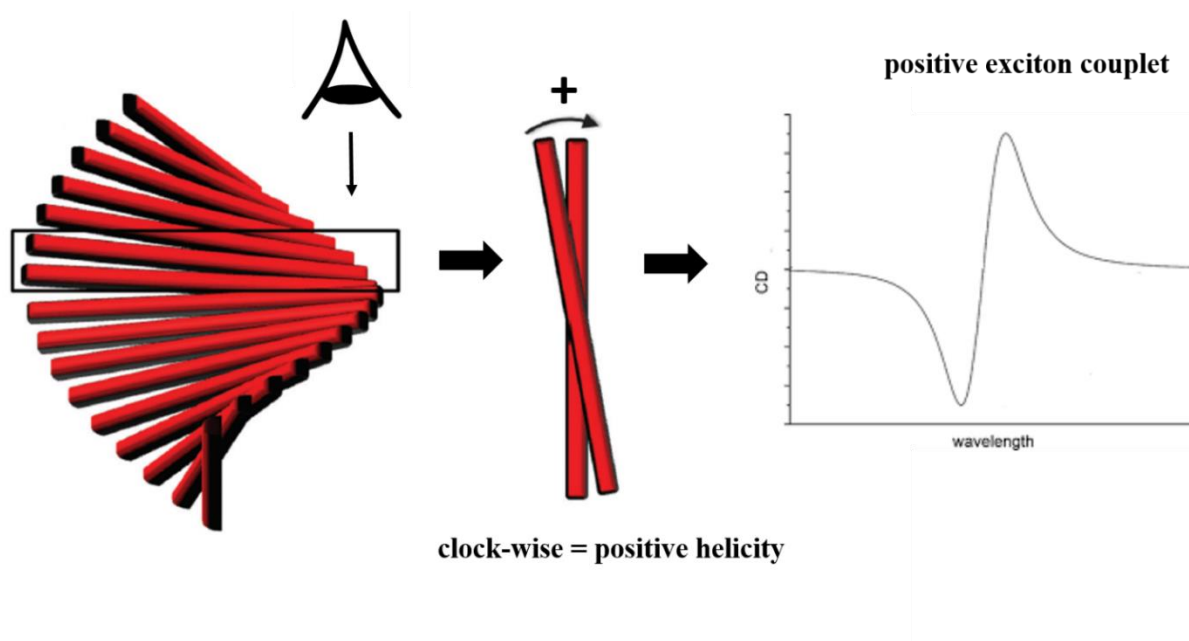


Figure 7. Example of aggregate with positive helicity and CD exciton couplet associated to it. The chirality of a dimer depends on the sense of rotation swept to superimpose with minimum angle the front dipole moment onto the one on the back. Clock-wise sense defines positive chirality and anticlock-wise negative.³⁹

It is important not to forget that Circular Dichroism is by definition the differential Absorbance of left-handed and right-handed circularly polarized light, that is $CD = A_L - A_R$. CD signal is therefore possibly non-vanishing only in proximity of absorption bands. A useful derived quantity is the g -factor (anisotropy or dissymmetry factor), defined as:

$$g = \frac{A_L - A_R}{A}$$

The anisotropy factor, not depending on concentration (unless for its influence on the aggregate itself) or pathlength, can help to quantify the chiral order degree in supramolecular aggregates. Thus, different molecules and samples can be compared with each other through this factor.³⁹

In fluorescent chiral aggregates, Circular Polarized Luminescence (CPL) can be detected. The measured quantity is the differential emission of left-handed and right-handed circularly polarized

light, $CPL = I_L - I_R$. Similarly to CD spectroscopy, a luminescence anisotropy factor can be defined:⁴³

$$g_{lum} = \frac{I_L - I_R}{\frac{1}{2}(I_L + I_R)}$$

CPL measurements give information on the chirality of the excited states of the chromophores, resulting a technique complementary to CD. Furthermore, both of these experimental techniques (CD and CPL) have the potential of providing information concerning molecular dynamics and energetics that occur between the time of excitation and emission.

⁴³ J. P. Riehl, G. Muller., Circularly Polarized Luminescence Spectroscopy and Emission-Detected Circular Dichroism. In: N. Berova, P. L. Polavarapu, K. Nakanishi, R. W. Woody, *Comprehensive Chiroptical Spectroscopy Vol. 1*, Wiley, 2012, 65-90.

1.4 Naphthalene Diimides: Characteristics and Applications

1,4,5,8-Naphthalene diimides (NDIs) are aromatic and chemically stable compounds, frequently investigated for their appealing properties for organic electronics. They are part of the aromatic diimides family shown in Figure 8.

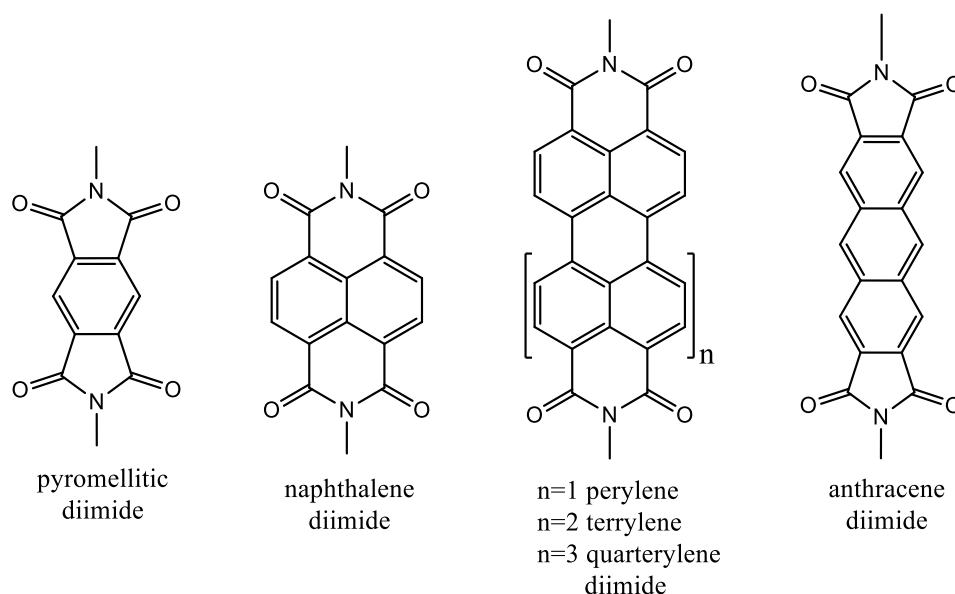


Figure 8. Aromatic diimides general structure.

All the aromatic diimides are capable to self-assemble through π - π stacking interactions in suitable conditions and their opto-electronic properties are strictly related to their supramolecular arrangement which can be tuned by nitrogen and core-substituents. Generally, the NDIs aromatic core has electron-deficient characteristics because of the four carbonyls of imide functionalities, allowing the molecule to undergo single one-electron reduction to form stable radical anion.⁴⁴ In this sense, NDIs are useful units to study photo-induced electron transfer mechanisms,⁴⁵ and can act as n-type semiconductors.

Naphthalene diimide core is usually soluble in low polarity lipophilic solvents (CHCl_3 , toluene) but groups directly bonded to nitrogen are crucial to determine solubility and therefore the aggregation behaviour. Simple alkyl chains improve the solubility in organic media, but also more

⁴⁴ G. Andric, J. F. Boas, A. M. Bond, G. D. Fallon, K. P. Ghiggino, C. F. Hogan, J. A. Hutchison, M. A. P. Lee, S. J. Langford, J. R. Pilbrow, G. J. Troup, C. P. Woodward, *Australian Journal of Chemistry*, **2004**, *57*, 1011–1019.

⁴⁵ S. Alpa, S. Ertena, C. Karapire, B. Köz, A. O. Doroshenko, S. Içli, *Journal of Photochemistry and Photobiology A: Chemistry*, **2000**, *135*, 103–110.

polar substituents have been extensively used to improve solubility in more polar media (DMF, MeOH, H₂O).⁴⁶

Substitution of NDIs core can have big influence on the optical properties. More electron-withdrawing groups enhance the π -acidity, improving π -stacking and π -anion interactions. In monomeric state, unsubstituted NDIs are usually not coloured nor fluorescent in the visible range. Core-substituted systems instead show absorption and emission spectra strongly depending on the nature of substituents, spanning the whole visible spectrum (Figure 9). In addition to NDI π - π^* transition in the range 300-400 nm, a new charge-transfer band between core-substituents and imide chromophores was observed in the visible range, going to red with increasing of the pull-push effect.

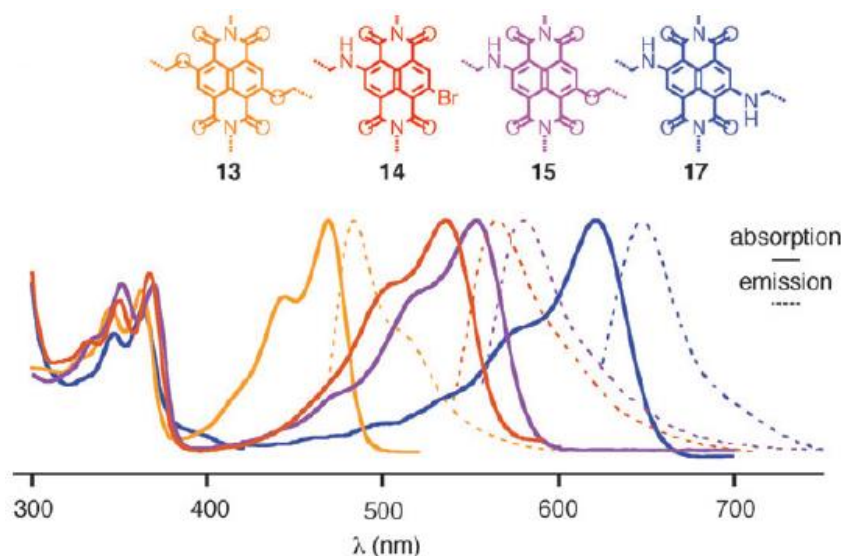


Figure 9. Absorption (solid line) and emission spectra (dashed line) of core-substituted NDIs⁴⁷

Several different supramolecular architectures can be obtained depending on the groups bonded to the imide functionalities: nanotubes, nanoparticles,⁴⁸ β -sheets⁴⁹. Quite common is the use of groups that can form H-bonding, in order to stabilize and direct self-assembly in the desired direction. An interesting example concerns simple acid-functionalized NDIs synthesised in Suhrith Ghosh's group.⁵⁰

⁴⁶ M.Kumar, S. J. George, *Nanoscale*, **2011**, 3, 2130-2133.

⁴⁷ R. S. K. Kishore, O. Kel, N. Banerji, D. Emery, G. Bollot, J. Mareda, A. Gomez-Casado, P. Jonkheijm, J. Huskens, P. Maroni, M. Borkovec, E. Vauthey, N. Sakai and S. Matile, *J. Am. Chem. Soc.*, **2009**, 131, 11106-11116.

⁴⁸ N. Ponnuswamy, G. D. Pantos, M. M. J. Smulders, J. K. M. Sanders, *J. Am. Chem. Soc.*, **2012**, 134, 566-573.

⁴⁹ H. Shao, T. Nguyen, N. C. Romano, D. A. Modarelli, J. R. Parquette, *J. Am. Chem. Soc.*, **2009**, 131, 16374-16376.

These molecules (Figure 10) can self-assemble in CHCl₃/methylcyclohexane mixtures giving novel emission properties, which are preserved in thin films. The emission spectra showed a broad emission band spanning almost the whole visible range and were attributed to the formation of excimer species pre-induced by aggregation. The aggregation could be stopped by addition of methanol, indicating that H-bonding were actually responsible for the features observed. It is also worth to note that small changes, like the length of the alkyl spacer between acid and imide functionalities, resulted in big changes in the supramolecular structure, which result in different light emission colors. Almost white emission has been observed for n = 1 and 3, and cyan and light yellow emission for n = 2 and n = 4 respectively. White emission in particular, is quite uncommon for a single organic chromophore.

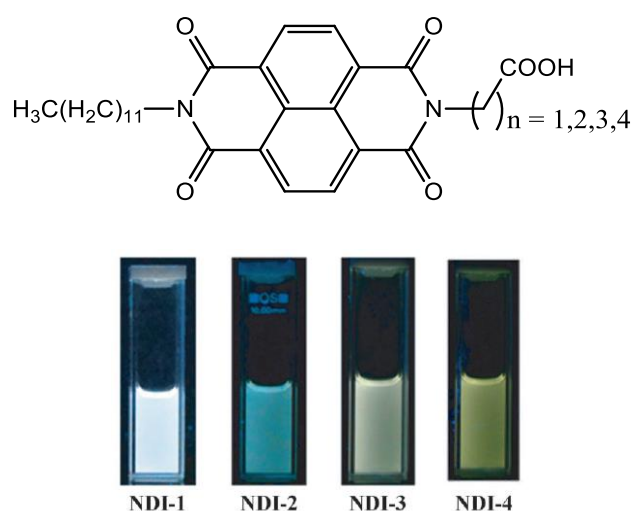


Figure 10. Structure of the acid-appended NDIs (top). Images of NDIs with different spacer lengths, in solution CHCl₃/MCH 5/95 under UV-lamp (bottom).

Computational studies proposed that a possible favourable aggregation mode of carboxylic acid functionalized NDIs is the formation of *syn-syn catemer* structure (Figure 11).^{50,51} Compared with more common formation of carboxylic acid dimers, the energy of this structure resulted minimized due to chain H-bonding and π -stacking interactions. In this proposed structure, the dodecyl alkyl chains did not result interdigitated to each other.

⁵⁰ M. R. Molla, D. Gehrig, L.Roy, V. Kamm, A. Paul, F.Laquai, S.Ghosh, *Chem. Eur. J.*, **2014**, *20*, 760 – 771.

⁵¹ J. N. Moorthy, R. Natarajan, P Mal, P. Venugopalan, *J. Am. Chem. Soc.*, **2002**, *124*, 6530-6531.

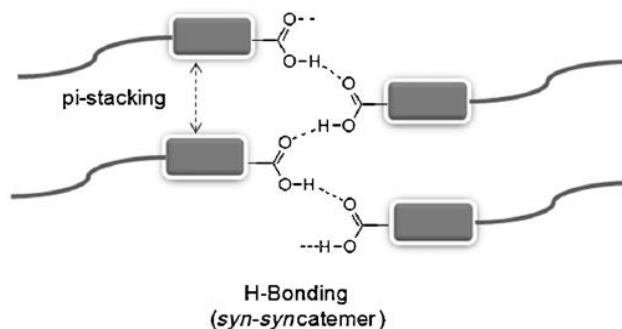


Figure 11. Proposed aggregation mode of acid-appended NDIs. π - π stacking and hydrogen bonding cooperate to form supramolecular structures.

Organic Electronics Applications

Organic π -conjugated semiconducting materials are currently under strong investigation for their use in electronic devices. Their ability to self-assemble in solid state by π -stacking, assure good intermolecular π orbitals overlap which facilitate charges mobility, resulting in good semiconductive properties. Some interesting characteristics of these organic systems are:⁵⁴

- I. Aromatic core electron-deficiency determine a good electron affinity and high electron mobility required in n-type semiconductors.
- II. Depending on their orbitals energy level, NDIs can be air-stable in many device operation conditions
- III. Compared with their higher homologues (rylenes), NDIs are more easily synthesisable and solution processable.

In this class of molecules, air-instability in electronic devices is due to vulnerability of the corresponding radical anions to reaction with water and oxygen. Air-stability can be improved by core substituents which modify the lowest unoccupied molecular orbital (LUMO) energy level of the molecule. Approximately, energy of LUMO should lie below -4 eV with respect to vacuum, to stabilize charge carriers from water and oxygen reduction (see Figure 12). Ideally, Oxygen and water molecules can be excluded by utilizing crystalline materials with sufficiently dense molecular packing to resist penetration by these species. Since π -orbital wave functions in these systems form nodes at the two nitrogen positions in the diimide rings⁵², N-substituents do not influence electronic properties significantly. However it was noted that substituents on nitrogen can have drastic effect on

⁵² H. E. Katz, A. J. Lovinger, J. Johnson, C. Kloc; T. Siegrist, W. Li, Y.-Y. Lin, Y.-Y., A. Dodabalapur, *Nature* **2000**, *404*, 478.

the packing and therefore on the air-stability and charge mobility of the material. Perfluorinated alkyl chains can lead to 10^3 - 10^5 times enhancement of the charge mobility in air.⁵³

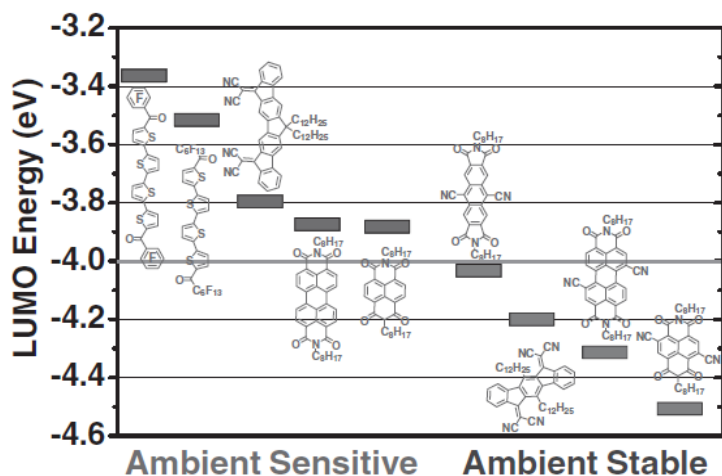


Figure 12. LUMO energy versus ambient stability correlation for OFETs based on several organic electron-transport materials.⁵⁴

Another example is the improvement given by a cyclohexyl ring directly bonded to nitrogen compared with linear alkyl chains, reported by Shukla et al.⁵⁵ (Figure 13). Rigid cyclohexyl chair-conformation assist intermolecular π - π stacking, affording an increase in charge mobility from 0.70 to $6.2 \text{ cm}^2 \text{ V}^{-1} \text{ s}^{-1}$ in Organic Thin-Film Transistor (OTFT), measured in vacuum.

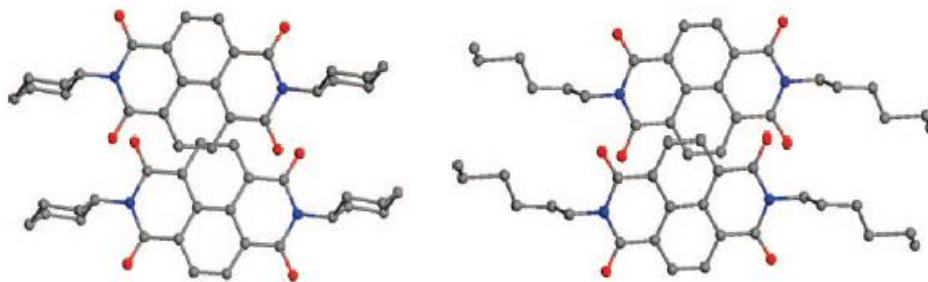


Figure 13. Crystalline packing for N,N'-cyclohexyl substituted NDI (left), and N,N'-hexyl substituted NDI.⁵⁵

Further recent applications of NDI based materials concern Organic Solar Cells. In a photovoltaic cell, the light passing through the transparent contact (typically indium tin oxide, ITO) is absorbed in the active layer to form excitons (hole-electron pairs), which dissociate into free

⁵³ H. E. Katz, J. Johnson, A. J. Lovinger, W. Li, *J. Am. Chem. Soc.*, **2000**, *122*, 7787.

⁵⁴ X. Zhan, A. Facchetti, S. Barlow, T. J. Marks, M. A. Ratner, M. R. Wasielewski, S. R. Marder, *Advanced Materials*, **2011**, *23*, 268-284.

⁵⁵ D. Shukla, S. F. Nelson, D. C. Freeman, M. Rajeswaran, W. G. Ahearn, D. M. Meyer, J. T. Carey, *Chem. Mater.*, **2008**, *20*, 7486-7491.

charges at the interface between the donor and the acceptor materials. Holes and electrons flow in the donor and acceptor regions, respectively, and are collected at the electrodes, resulting in the generation of electrical power (general operating principle is shown in Figure 14). The components have to be chosen suitably to optimize several parameters, including the acceptor HOMO-LUMO band gap, and the LUMO energies difference between donor and acceptor.

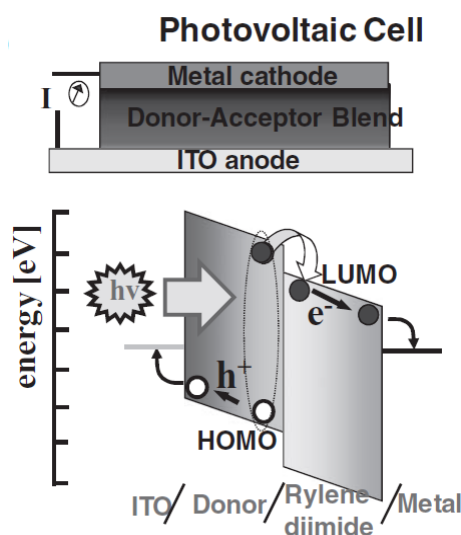


Figure 14. OPV cell material components (top) and energetics of the light absorption and charge-collection processes involving a rylene diimide as the acceptor material. The energy level diagram of the donor/acceptor interface shows photoexcitation of an electron into the LUMO of the donor followed by the electron transfer into the acceptor LUMO and migration of the separated charges away from the interface.⁵⁴

p-conducting polymers like polythiophenes⁵⁶ are commonly used as donor materials. Most employed acceptor materials are currently fullerenes derivatives.⁵⁷ However, they have drawbacks, including a low absorption in the visible-NIR range and scarce control over their HOMO and LUMO energy levels. Rylene-based acceptor oligomers and polymers allow one to avoid these drawbacks, and their band gap can be tuned by core and nitrogen substituents as described above.

Organic Light Emitting Diodes are another possible application for organic materials which present emitting properties. So far, efficient electroluminescence was obtained from various perylene diimides (PDI) aggregates.^{58,59} On the other hand, emitters based on NDI supramolecular structures remain rather uncommon and need to be explored further.⁶⁰

⁵⁶ B. Fan, P. Wang, L. Wang, G. Shi, *Solar Energy Materials & Solar Cells*, **2006**, *90*, 3547–3556.

⁵⁷ Y. He, Y. Li, *Phys. Chem. Chem. Phys.*, **2011**, *13*, 1970–1983.

⁵⁸ E. I. Haskal, Z. Shen, P. E. Burrows, S. R. Forrest, *Physical Review B*, **1995**, *51*, 4451–4463.

⁵⁹ F. J. Céspedes-Guirao, S. García-Santamaría, F. Fernández-Lázaro, A. Sastre-Santos, H. J. Bolink, *J. Phys. D: Appl. Phys.*, **2009**, *42*, 105–106.

⁶⁰ Y. Ofir, A. Zelichenok, S. Yitzchaik, *J. Mater. Chem.*, **2006**, *16*, 2142–2149.

1.5 Chirality in Organic Electronic Devices

A recent research field in organic electronics is the application of chiral molecules in order to obtain new opto-electronic properties. Circularly polarized (CP) light is currently exploited in circularly polarized ellipsometry-based tomography,⁶¹ efficient LCD backlights,⁶² optical quantum information and data storage.⁶³ To optimize these technologies, compact and low-cost devices which avoid the use of polarizing filters would be ideal. In this sense, organic chiral molecules could fulfill these requirements, being able to emit and detect circularly polarized light and are currently under strong investigation. Recent examples of applications of chiral organic molecules in these fields are the first non-racemic helicene-based OFET and OLED^{64,65} (Figure 15).

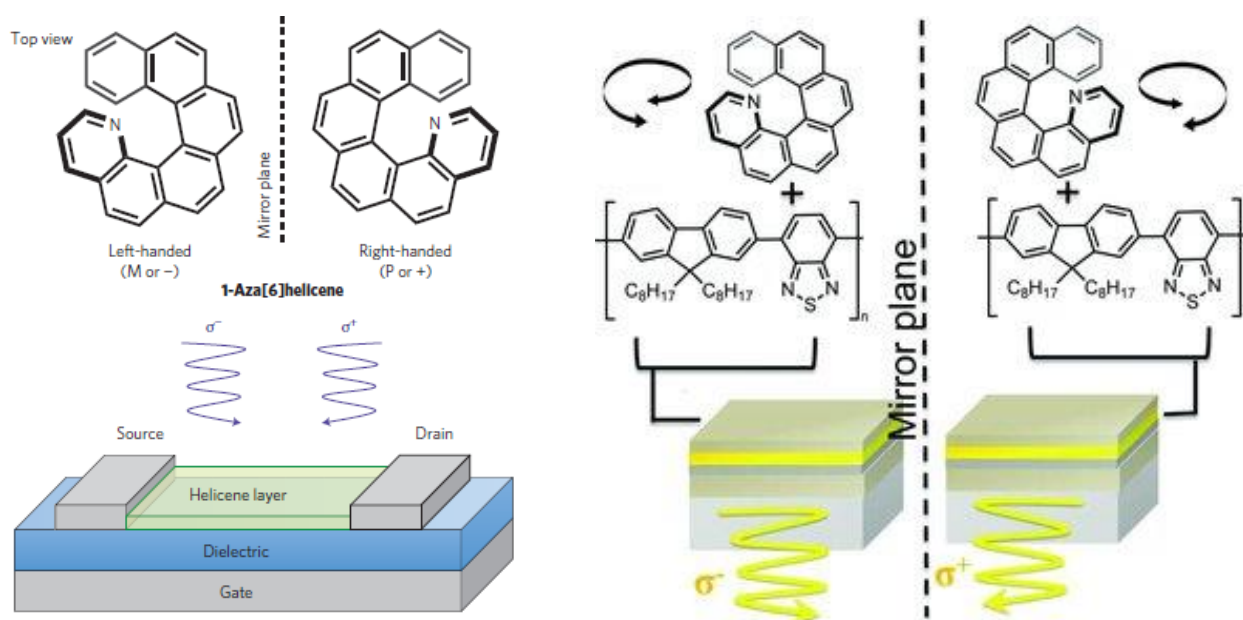


Figure 15. Schematic representation of OFET (left) and CP-OLED (right) based on 1-aza[6]helicene. Figures adapted from references 64 and 65.

In the OFET, an enantiomerically pure 1-aza[6]helicene layer was used as semiconductor to detect circularly polarized light. The resistance of the device measured when irradiated by circularly polarized light was directly related to the absolute configuration of the helicene. The specific photoresponse obtained, depended on the selective absorption of the circularly polarized light from the active layer. Therefore, organic semiconductors with high g are required to have good response

⁶¹ C. J. Yu, C. E. Lin, L. P. Yu, C. Chou, *Appl. Optics*, **2009**, *48*, 758–764.

⁶² M. Schadt, *Annu. Rev. Mater. Sci.* **1997**, *27*, 305-379.

⁶³ C. Wagenknecht, C.-M. Li, A. Reingruber, X.-H. Bao, A. Goebel, Y.-A. Chen, Q. Zhang, K. Chen, J.-W. Pan, *Nat. Photonics* **2010**, *4*, 549.

⁶⁴ Y. Yang, R. Correa da Costa, M. J. Fuchter, A. J. Campbell, *Nature Photonics*, **2013**, *7*, 634–638.

⁶⁵ Y. Yang, R. Correa da Costa, M. J. Fuchter, D.-M. Smilgies, A. J. Campbell, *Adv. Mater.*, **2013**, *25*, 2624–2628.

selectivity. The electroluminescent polymer-based OLED doped with enantiomerically pure 1-aza[6]helicene, showed highly circularly polarized emission. The common electroluminescent devices employing polarizing filters could be substituted with intrinsic CP-OLED, obtaining less expensive and bulky devices. To do this, high g_{lum} values of the organic emitter are needed. As further example, in our group the first lanthanide-based CP-OLED was built, which showed the highest electroluminescence anisotropy factor ever obtained for an OLED (± 0.75).⁶⁶

Another recent application of chiral organic molecules involves the electron spin polarization in semiconducting materials. The Spintronics is the branch of electronics in which electron spin, in addition to its charge, is manipulated to yield a desired outcome.⁶⁷ Naaman's group recently established experimentally and theoretically the Chiral-Induced Spin Selectivity effect (CISS).⁶⁸ According to this effect, the spin states of electrons flowing in an external chiral electrostatic field are no more degenerate, due to effective magnetic field generated by the electrons movement itself. Since the electrons with disadvantaged spin are slowed down or scattered, molecules in chiral arrangement can actually act as spin 'filter', allowing only electrons with favourite spin to flow through the material (Figure 16).

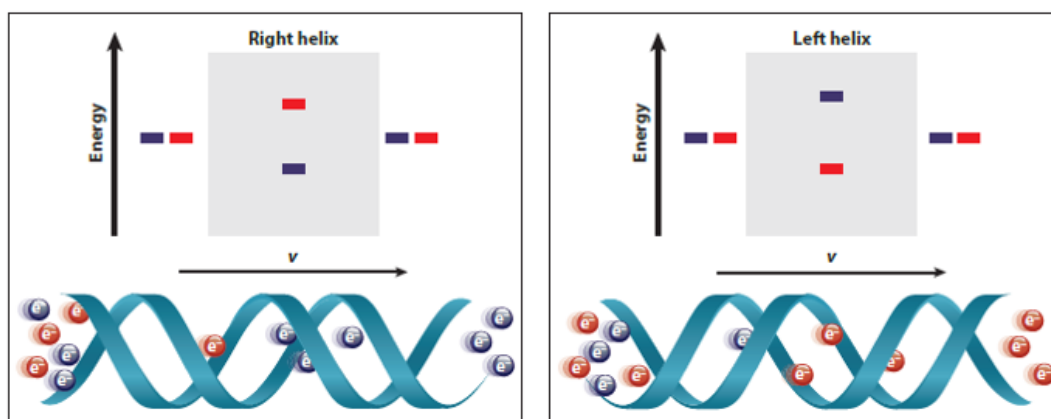


Figure 16. Schematic representation of the chiral-induced spin selectivity effect. Electrons with opposite spins are represented in red (spin up) and blue (spin down), flowing through left-handed and right-handed helical molecule. The spin orientation of the electrons prefers to be aligned parallel or antiparallel to their velocity, depending on the handedness of the chiral electrostatic potential.⁶⁹

As a result, the electrical resistance of an electronic device can be varied depending on the chirality of the semiconducting layers. So far, chiral organic spin filters have been built and tested exploiting

⁶⁶ F. Zinna, U. Giovanella, L. Di Bari, *Adv. Mater.*, **2015**, *27*, 1791–1795.

⁶⁷ S. A. Wolf, D. D. Awschalom, R. A. Buhrman, J. M. Daughton, S. von Molnár, M. L. Roukes, A. Y. Chtchelkanova, D. M. Treger, *Science*, **2001**, *294*, 1488-1495.

⁶⁸ R. Naaman, D. H. Waldeck, *J. Phys. Chem. Lett.*, **2012**, *3*, 2178–2187.

⁶⁹ R. Naaman, D. H. Waldeck, *Annu. Rev. Phys. Chem.* **2015**, *66*, 263–281.

the natural chiral pool.^{70,71} In future, many common spintronic devices, which currently exploit inorganic materials and external magnetic fields to control spin polarization (Hard Disk in personal computers for example), could be substituted by low-cost and easier processable chiral organic molecules.

⁷⁰ M. Kettner, B. Göhler, H. Zacharias, D. Mishra, V. Kiran, R. Naaman, C. Fontanesi, D. H. Waldeck, S. Şek, J. Pawłowski, J. Juhaniewicz, *J. Phys. Chem. C*, **2015**, *26*, 119-124.

⁷¹ B. Göhler, V. Hamelbeck, T. Z. Markus, M. Kettner, G. F. Hanne, Z. Vager, R. Naaman, H. Zacharias, *Science*, **2011**, *331*, 894-897.

Aim of the Thesis

Organic supramolecular materials are promising candidates for electronic applications. However, few examples of chiral self-assembled architectures employed in spintronics and circularly polarized-based devices, are reported in literature. Our purpose was to investigate the chiroptical properties of some simple π -conjugated systems upon self-assembly, in order to contribute to this new stimulating research field. Among the numerous aromatic systems known, we chose the chiral naphthalene diimide (NDI) derivatives as target molecules for this work. This choice depended on the good semiconducting and self-assembly properties of the NDI derivatives, already exploited in organic electronics. We designed three easy synthesizable molecules bearing different functional groups (carboxylic acid, amide and alkyl chain), in order to investigate the differences among them on a supramolecular chirality level (Figure 17). The chirality was assured by the same alkyl chain derived from the (S)-citronellol, a natural compound available enantiomerically pure.

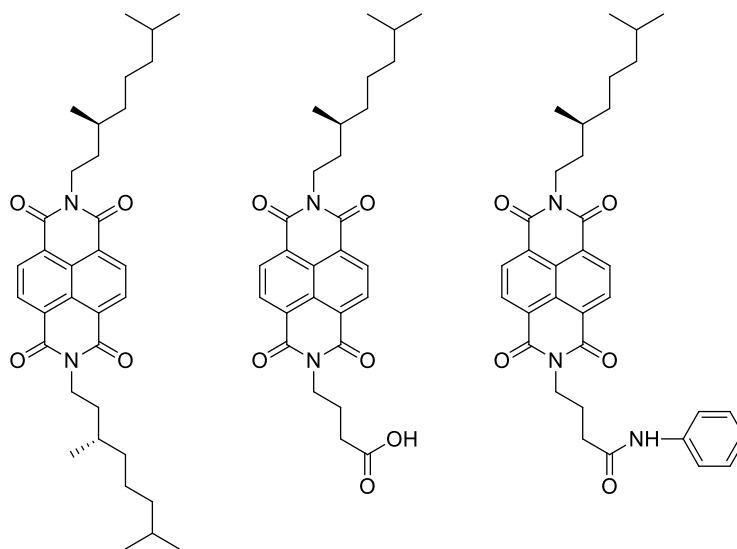


Figure 17. NDI derivatives synthesised in this work. NDI chromophore was connected on one side to the same chiral alkyl chain for all the three compounds. On the other side, the chiral alkyl chain, a carboxylic group and an amide group were connected, respectively.

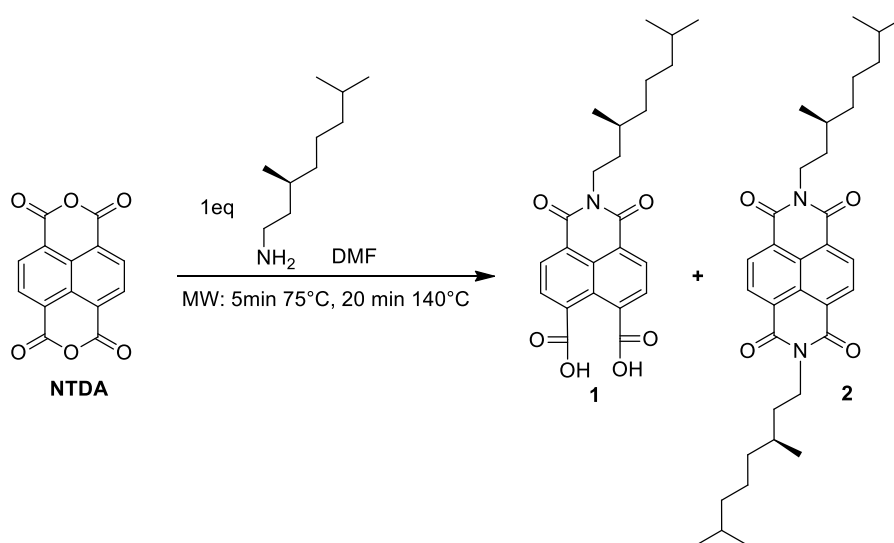
The supramolecular aggregates obtained were studied via optical and chiroptical spectroscopy, in order to understand their structure and opto-electronic properties. In particular, to apply these molecules in OFET-based chiral sensor, CP-OLED or spintronic devices, we aimed to obtain structures with high chiral order (that is high anisotropy factors) in solid state. Therefore, we investigated the behaviour of these molecules first in solution, and then as thin film, powder and crystals.

2 Results and Discussion

2.1 Synthesis and Characterization

2.1.1 Amine functionalization of naphthalene tetracarboxylic dianhydride (NTDA)

Keeping in mind the recent literature,⁷² we used a modified microwave-assisted procedure in two steps to synthesise N-desymmetrized naphthalene diimides starting from naphthalene tetracarboxylic dianhydride (NTDA). This procedure was planned to minimize the amount of bis N-substituted product usually found in one-pot methods⁷³ and purify the final product without intermediate purification. The first step is shown in Scheme 1. (S)-3,7-dimethyloctylamine was chosen as the chiral enantiopure building block. The amine was already synthesised in three steps starting from (S)-citronellol,⁷⁴ a commercial natural terpene.



Scheme 1. Synthetic procedure to **1** starting from NTDA. Side-product **2** was also obtained.

The reaction was carried out in DMF, aprotic polar solvent which features microwave absorption allowing homogeneous heating of the mixture. A pre-heating step at 75°C was performed to help the

⁷² K. Tambara, N. Ponnuswamy, G. Hennrich, G. D. Pantos, *J. Org. Chem.*, **2011**, 76, 3338-3347;

⁷³ P. Pengo, G. D. Pantos, S. Otto, J.K.M. Sanders, *J. Org. Chem.*, **2006**, 71, 7063-7066;

⁷⁴ T. Terashima, T. Mes, T. F. A. De Greef, M. A. J. Gillissen, P. Besenius, A. R. A. Palmans, E. W. Meijer, *J. Am. Chem. Soc.*, **2011**, 133, 4742-4745.

dissolution of the reagents. Then, a successive step at 140°C for 20 minutes was required. The work-up was performed removing DMF under reduced pressure, and washing the residue with basic water (NaOH 1M). At pH > 5-6 naphthalene monoimide (NMI) **1** and non-reacted NTDA are soluble in water thanks to anhydride hydrolysis and formation of two (respectively four) carboxylate functionalities per molecule, which allowed us to filter off the insoluble by-product **2**. Then aqueous HCl was added to the filtrate until pH 6 was obtained. More acidic solution can bring to precipitation of non-reacted NTDA. The white product **1** was then dried at 60°C under vacuum overnight and characterized (yield 47%).

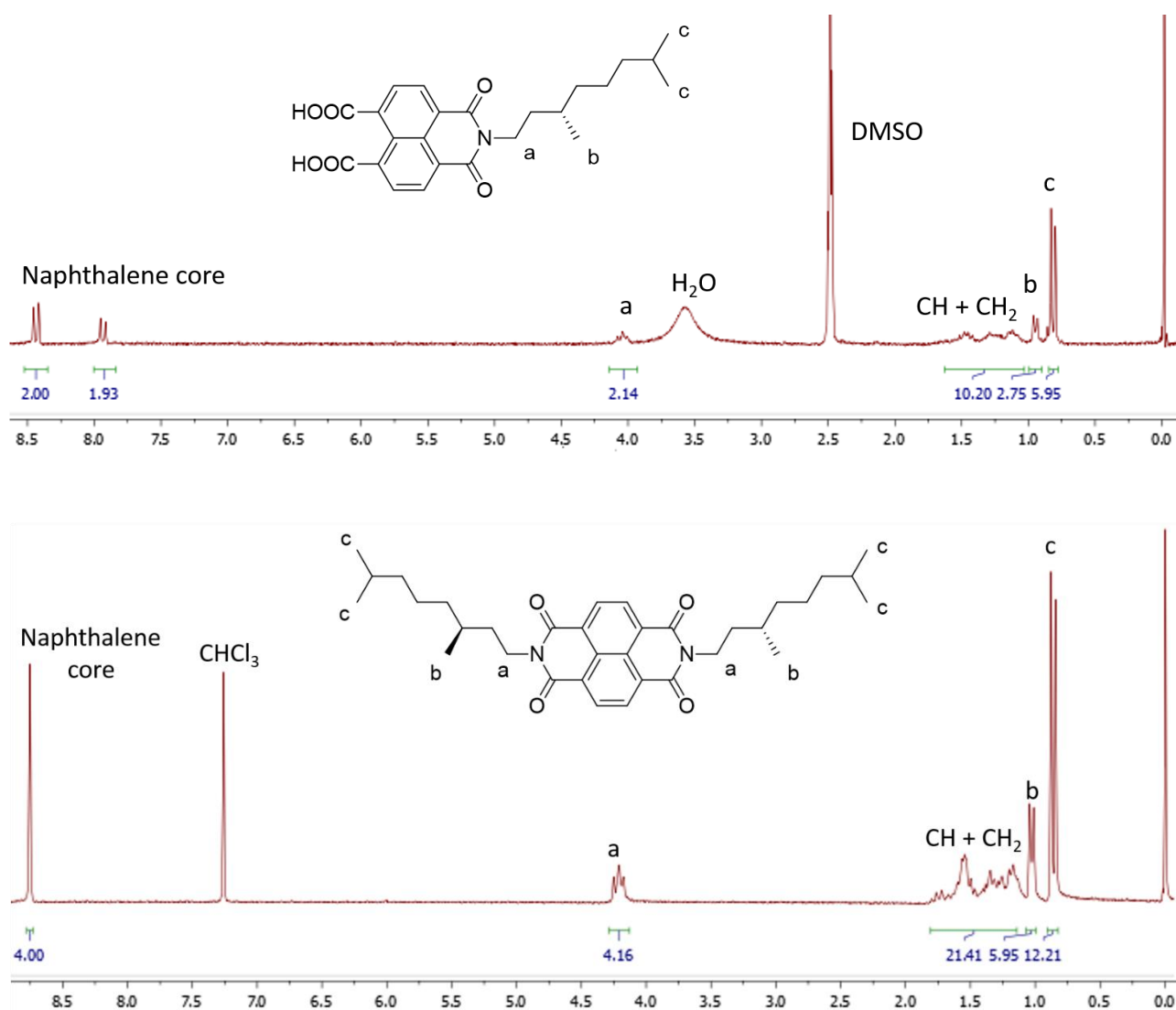
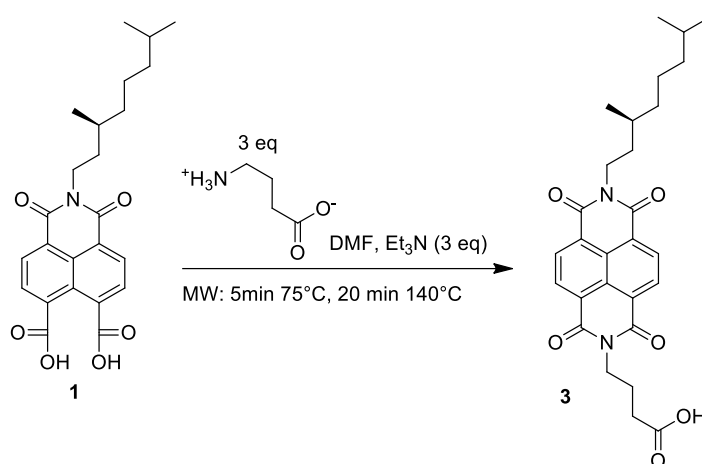


Figure 18. ¹H-NMR spectra (400 MHz) of compounds **1** in DMSO-d₆ (top) and **2** in CDCl₃ (bottom).

2.1.2 Synthesis of the naphthalene diimides

An amino acid was needed in order to obtain a NDI bearing a carboxylic group. The commercially available γ -aminobutyric acid, containing C₃-spacer between amino and acid functionalities was chosen. The same procedure described in the previous section was used to obtain the product **3** from the naphthalene monoimide **1** (Scheme 2). Since the amino acid was available as solid in zwitterionic form, a non-nucleophilic base was needed to deprotonate the ammonium group and make the nitrogen react with the NMI **1**. A stoichiometric amount of triethylamine was separately stirred with the amino acid before adding to the reaction mixture.



Scheme 2. Synthetic procedure to acid-appended NDI **3** starting from NMI **1**.

We found that for reaction scales bigger than 200 mg of **1**, the use of only 1 equivalent of γ -aminobutyric acid was not sufficient under these reaction conditions to obtain good conversion of the NMI **1**. This was probably due to the scarce solubility of the NMI **1** in DMF and the scarce reactivity of the nucleophile. However, when 3 equivalents of the amino acid were added to the mixture, the reaction resulted faster enough to obtain a good conversion.

The work-up was achieved through precipitation of the product **3** in slightly basic water. The solid was filtered, dried at 60°C under vacuum overnight and purified by chromatographic column (Chloroform/Methanol 95/5) to obtain acid **3** (yield 35%). ¹H-NMR analysis confirmed that no other byproducts were present in the solid after purification (Figure 19).

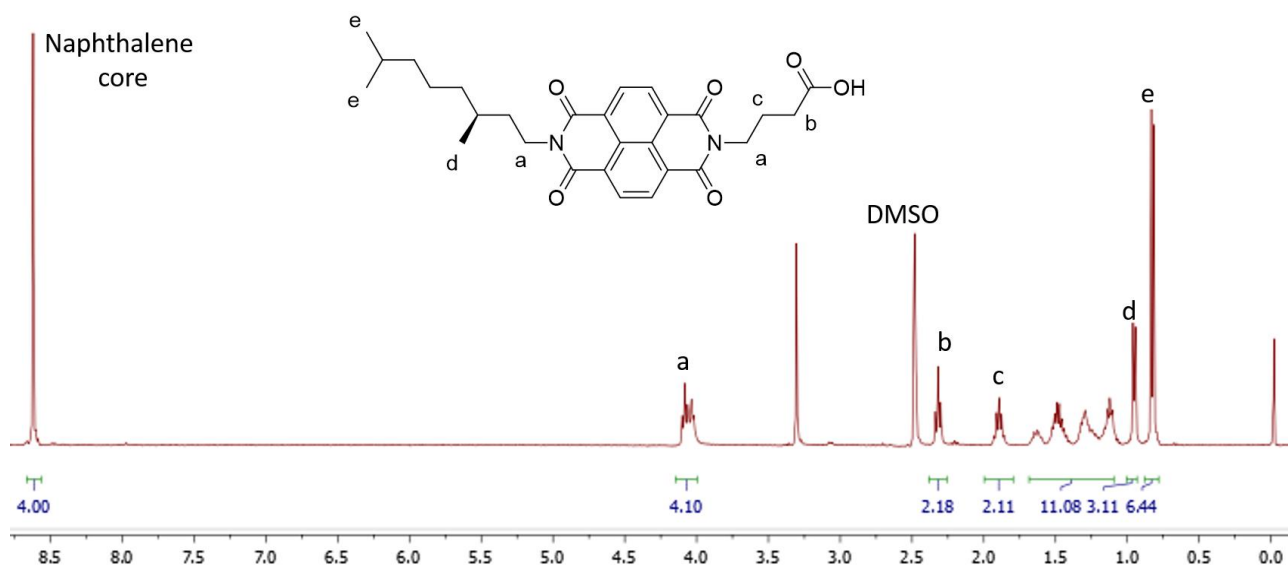
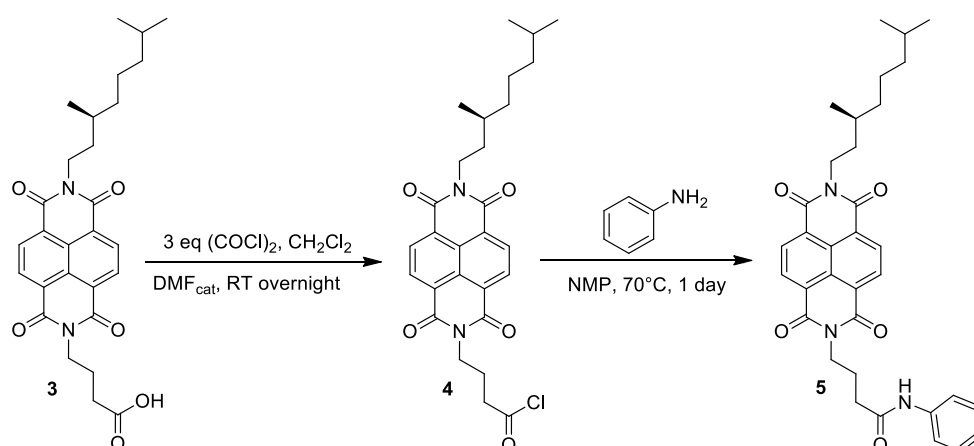


Figure 19. $^1\text{H-NMR}$ spectrum (400 MHz) of compound **3** (DMSO- d_6).

Since changes in molecular structure can give different self-assembly outcome, we decided to synthesise an amide-appended naphthalenediimide to investigate differences with acid **3** in the H-bonding role.

The same acid **3** was used to synthesise the amide **5** according to Scheme 3. Acid chloride **4** was obtained by addition of oxalyl chloride in excess and catalytic DMF under inert atmosphere. Since aniline could act as nucleophile and base catalyst as well, additional base was not required but aniline was added in excess (2.5 equivalents). The product was then purified by chromatography (Chloroform/Methanol 95/5) to obtain pure amide **5** (yield 28%). The $^1\text{H-NMR}$ spectrum is shown in Figure 20.



Scheme 3. Synthetic procedure to amide **5** starting from acid **3**.

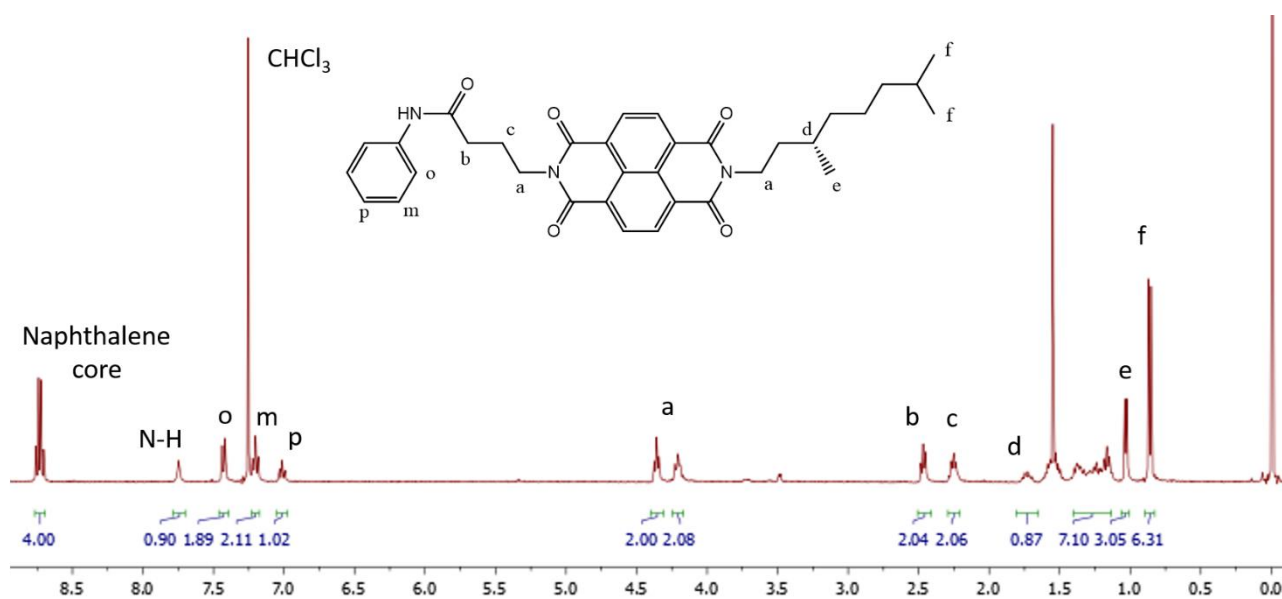


Figure 20. ¹H-NMR spectrum (400 MHz) of compound **5** (CDCl₃)

2.2 Thermal and Morphological Properties

Thermal behaviour of NDI derivatives including phase transitions was investigated by a combination of differential scanning calorimetry (DSC) and Polarized Optical Microscopy (POM). For DSC three heating/cooling cycles were performed from 20°C to 250°C for the compounds **3** and **5** and from 20°C to 180°C for compound **2**. For each compound a 10°C/min rate was used in the first two cycles and a faster 40°C/min in the third one. All the phase transitions are reported in Table 2.

Table 2. Melting and crystallization temperatures at 10°C/min and 40 °C/min heating/cooling rates for compounds **2**, **3** and **5**.

	T _{melt} / °C (1°/ 2° cycle) 10°C/min	T _{cryst} / °C (1°/ 2° cycle) 10°C/min	T _{melt} / °C 3° cycle 40°C/min	T _{cryst} / °C 3° cycle 40°C/min
2	168/168	153/147	169	147
3	225/223	218/215	224	188
5	225/226	196/197	224	214

A trivial observation is that molecules containing functional groups which can form hydrogen bonding have higher melting and crystallization point compared to NDI **2** containing only alkyl chains. No liquid crystalline behaviour was observed but under cooling a small transition could be observed for **2**, **3** and **5** in the range 60-70 °C. Since this effect was in common for all the three compounds, we suggested that it could be due to the stacking of the alkyl chains, which are identical for all of them.

POM analysis was applied to check DSC information and obtain more information about crystalline order. Samples were prepared spin-coating a concentrated solution in chloroform (10 mg/mL) on a glass surface, 60 seconds at 2000 rpm, in order to obtain an amorphous layer. The films were then heated at 10 °C/min above the melting point and cooled at the same rate to room temperature. Under cooling, **5** did not show any kind of solid state order. NDI **2** and **3** instead showed partially crystalline order below 80 °C and 130 °C respectively. POM view of the crystalline order for compounds **2** and **3**, are shown in Figure 21. Larger ordered domains were observed for acid functionalized NDI **2**.

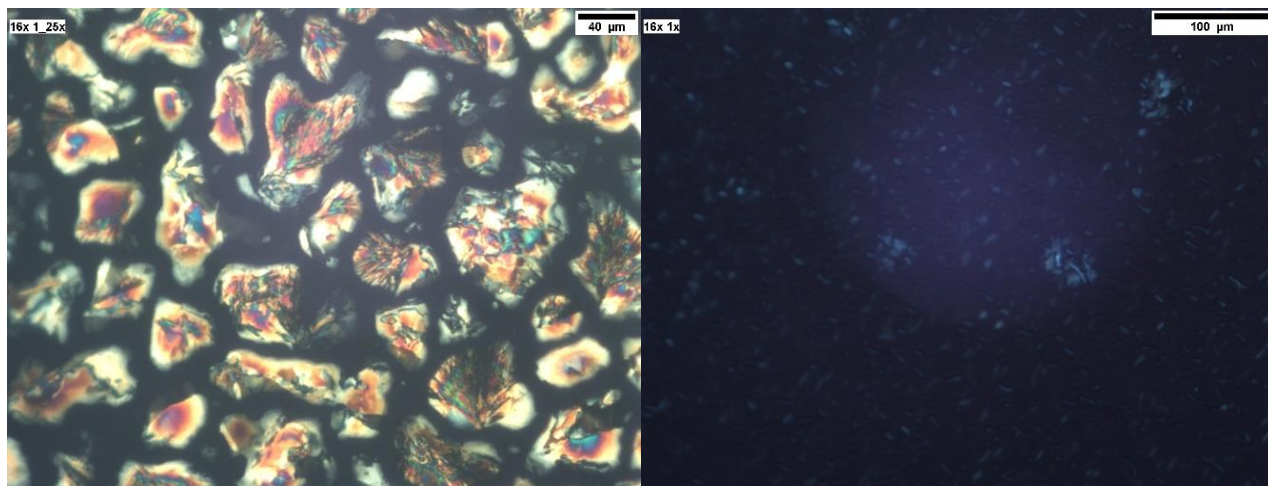


Figure 21. POM view of thin films for compounds **3** (left) and **2** (right) after heating and cooling cycle, RT. Bigger crystalline domains could be observed for compound **3**.

2.3 Characterization of the N,N'-dialkyl Naphthalene Diimide

2.3.1 Optical and chiroptical characterization in solution

As discussed in the introduction, naphthalenediimide (NDI) and perylenediimides (PDI) can form supramolecular aggregates in suitable conditions, usually triggered by bad solvents or low temperature. To investigate this behaviour, optical and chiroptical spectroscopy techniques were employed. In this section, the study of the naphthalene diimide **2** bearing the (S)-3,7-dimethyl alkyl chains on both sides will be described (Figure 22).

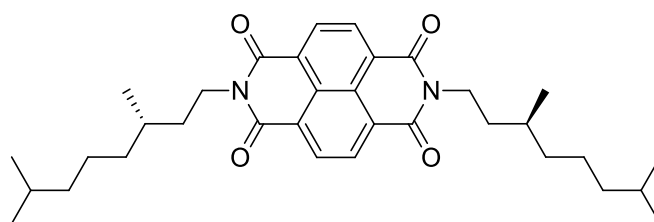


Figure 22. Structure of the chiral NDI **2** bearing two enantiopure alkyl chains.

Firstly UV-Vis spectrum of compound **2** was recorded in a good solvent. Etheral and Chlorinated solvents can efficiently solvate aromatic portions and alkyl chains as well. THF solution $5 \cdot 10^{-5}$ M of compound **2** showed the following spectrum, typical for monomeric non-interacting NDIs (Figure 23).

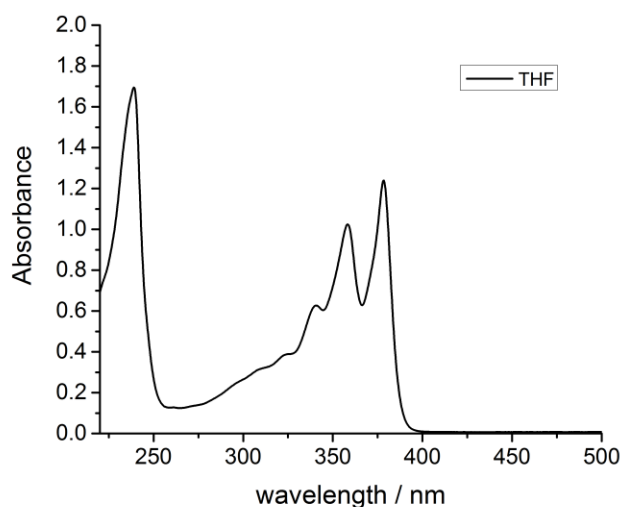


Figure 23. UV-Vis spectrum of compound **2** in THF. Concentration $5 \cdot 10^{-5}$ M, RT.

As reported in literature,⁷⁵ these absorption bands arise from naphthalenediimide long-axis (band I, 220-250 nm) and short-axis (band II, 300-400 nm) polarized transition dipoles (Figure 24), and have π - π^* character. Vibronic progression associated to the lower energy transition of the naphthalenediimide chromophore was observed (three maxima at 378, 358 and 340 nm).

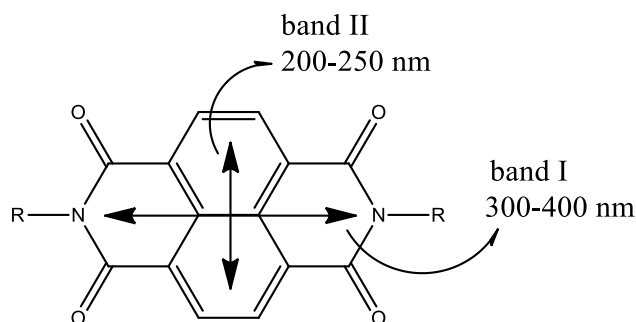


Figure 24. Short and long-axis polarized π - π^* dipole transition in naphthalene diimide chromophore.

In order to investigate the aggregation behaviour in solution, absorption spectra were recorded in different mixtures of 1,1,2,2-tetrachloroethane (TCE) and methylcyclohexane (MCH). Hydrocarbon solvents resulted non-effective to promote aggregation. In fact even in pure MCH, only a small hypsochromic shift due to solvatochromic effect was observed. MCH solution was then cooled to 5°C but no change in the spectra occurred. On the contrary, fluorescence experiments carried out in pure MCH at variable temperature showed a new aspect (Figure 25).

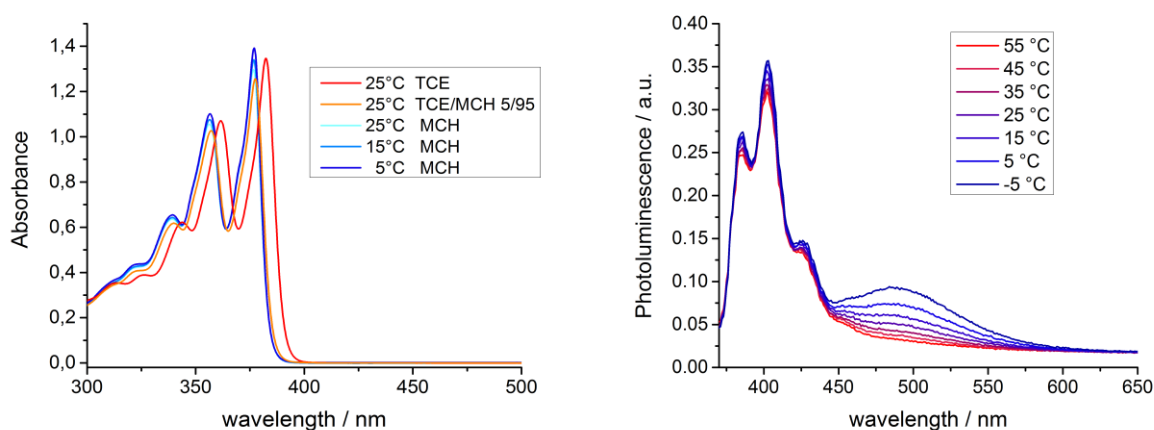


Figure 25. UV-Vis spectrum of compound **2** in different mixtures TCE/MCH at RT, and in MCH at variable temperature, concentration $5 \cdot 10^{-5}$ M (left). Emission spectra of compound **2** in MCH at variable temperature, concentration $5 \cdot 10^{-5}$ M (right).

The compound **2** was excited at 356 nm, the 0-1' transition. At 55°C only the mirror-image of the absorption spectrum of the monomer can be observed as expected. Below room temperature instead,

⁷⁵H. Shao, J. Seifert, N. C. Romano, M. Gao, J. J. Helmus, C. P. Jaroniec, D. A. Modarelli, J. R. Parquette; *Angew. Chem. Int. Ed.* **2010**, *49*, 7688–7691

a new weak emission band centred at 485 nm could be seen. Since no evidence for aggregation at ground state came from absorption spectra and the new band looked quite broad and unstructured, we could definitely associate this effect to excimer fluorescence.^{76,77}

Another attempt to induce aggregation was carried out employing different volume fractions of water as bad solvent, in THF. In pure THF, as already described, the compound **2** is molecularly dissolved. When the mixture is composed by 50% of water, significant change in the absorption spectrum can be observed. UV-Vis spectra reported in Figure 26 showed the rising of a new red-shifted peak at 396 nm with decreasing of monomer band I at the same time. Band II exhibited also red-shift for mixtures containing more than 50% of water with highest intensity for the mixture THF/H₂O 30/70. According to literature these effects indicate the formation of aggregates in solution.⁴⁶

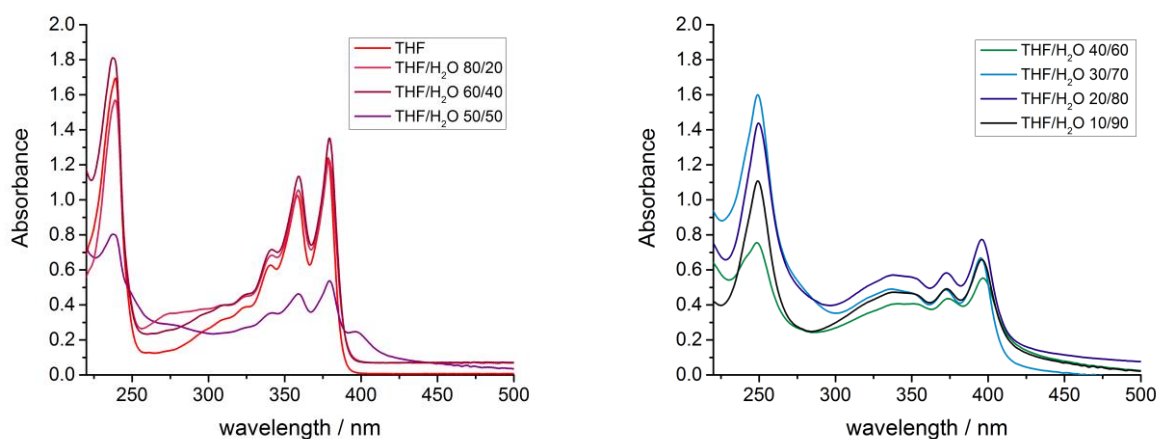


Figure 26. UV-Vis spectra of compound **2** in different mixtures THF/H₂O. From 0 to 50 % of water (left), from 60 to 90 % of water (right), concentration $5 \cdot 10^{-5}$ M, RT.

Fluorescence spectroscopy could give more information about this new type of aggregates. Below 50% of water, there is no appreciable aggregate emission in the range 400–600 nm. For water volume fractions equal to or higher than 50% instead a new much more intense band with λ_{max} around 455 nm could be detected. This new band was broad and showed a shoulder at 420 nm. Blue emission could be visually seen for all these mixtures measured. Increasing the amount water, a slight redshift from 455 to 459 nm for the maximum was observed but total emission intensity reached a maximum with 60% of water. Emission spectra and pictures of fluorescent samples are shown in Figure 27. Decreasing of the fluorescence intensity above 60% of water, could be due to several effects: the precipitation of the aggregates over time or the formation of a different kind of less emissive aggregate. The broad emission band suggested an excimer-like character as previously reported for

⁷⁶ J. B. Birks, *Nature*, **1967**, 214, 1187-1190.

⁷⁷ T. Förster, *Angew. Chem. internut. Edit.*, **1969**, 8, 333-343.

NDI derivatives dissolved in polar solvents.⁷⁸ However, UV-Vis spectra showed that red-shift effect occurred already in the ground electronic state, indicating that the excimer fluorescence is pre-induced by self-assembled structure.

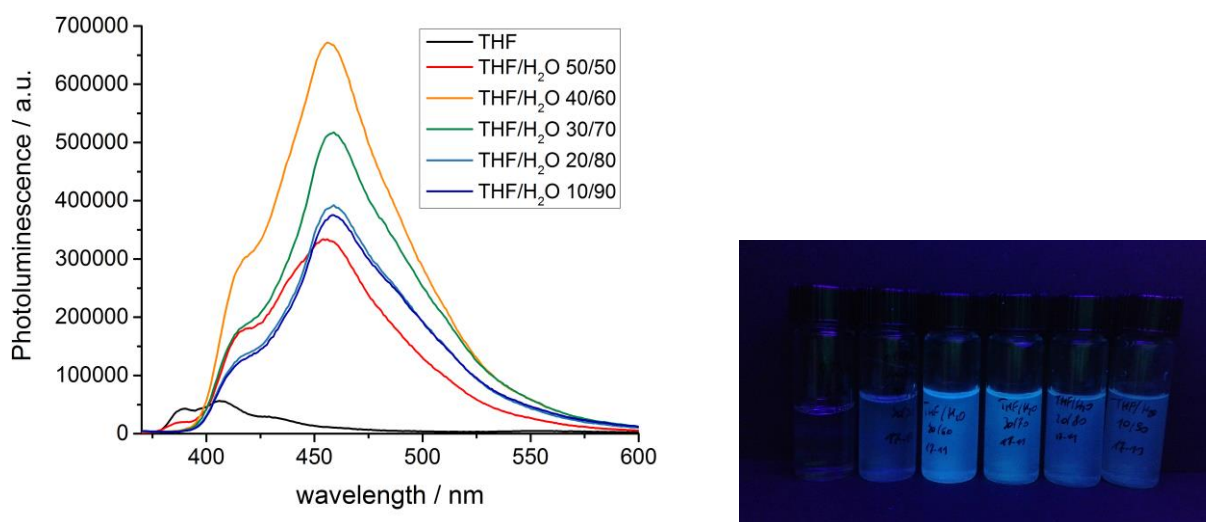


Figure 27. Emission spectra of compound **2** in different mixtures THF/H₂O. Excitation wavelength 356 nm. Concentration $5 \cdot 10^{-5}$ M, RT (left). Photo of mixture used for measurements under UV lamp irradiation, from left to right: 0, 50, 60, 70, 80, 90 % of water in THF, RT (right).

Taking advantage of enantiopure chiral alkyl chains connected to the aromatic chromophore, Circular Dichroism spectroscopy was performed to assess chiral order in these supramolecular structures. Different THF/H₂O mixtures were analysed as already done for UV-Vis spectroscopy. Consistently with absorption spectra shown in the previous paragraph, 50% of water was needed to induce self-assembly (Figure 28). Increasing the amount of water, Cotton effect for both band I and II was observed. The mixture THF/H₂O 50/50 showed negative Cotton effect for both band and scattering can be noted in the form of tail at high wavelengths. Increasing the amount of water, the band II reached the maximum magnitude of CD signal at 70% of water, and a pure negative exciton couplet can be seen. Band I instead changed going from a bisignate negative signal for 60% of water, to a weak positive couplet for 90% of water. This spectra evolution suggested that at least two different types of supramolecular structures can be possible varying solvent composition. Sign of the exciton couplet at 250 nm and of band I suggested that, below 90% of water, both short- and long-axis polarized transition dipoles are oriented in a left-handed M-type helical arrangement.⁷⁹ However with 90% of water, a clear handedness of aggregates could not be defined. An additional

⁷⁸ M. Pandeeswar, M. B. Avinash, T. Govindaraju, *Chem. Eur. J.*, **2012**, *18*, 4818 – 4822.

⁷⁹ J. Gawronski, M. Brzostowska, K. Kacprzak, H. Kolbon, P. Skowronek, *Chirality*, **2000**, *12*, 263.

explanation of CD weakening can be again the increasing of hydrophobic effects: too high water fraction forces the aggregates to be more compact with resulting decreasing of the supramolecular chirality degree.

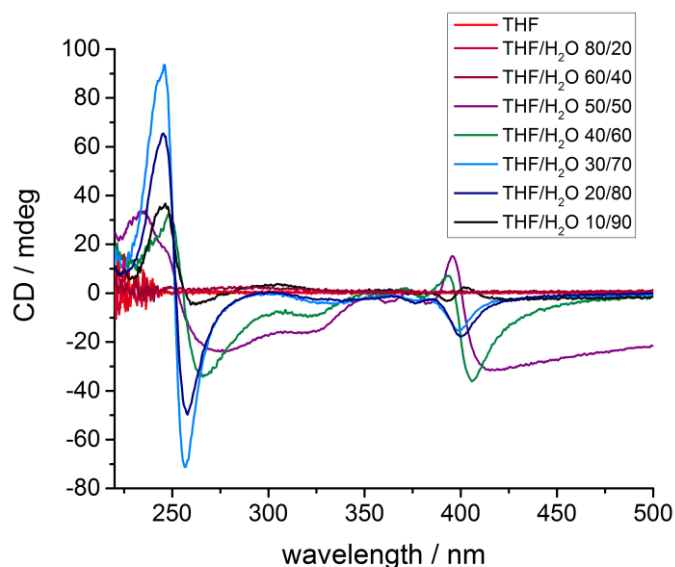


Figure 28. CD spectra of compound **2** in different mixtures THF/H₂O, concentration $5 \cdot 10^{-5}$ M, RT.

In the end, CD spectroscopy resulted useful giving additional information about the handedness of the aggregates that were not accessible through standard optical spectroscopy.

To assess chirality of excited state in NDI **2**, Circularly Polarized Luminescence spectroscopy was applied to the mixtures which showed detectable signal. Solutions were irradiated with a UV light centred at 360 nm. Circularly polarized emission was detected for the broad emission band originated from aggregates in the 400-550 nm range. THF/H₂O mixtures containing at least 50% of water showed detectable CPL signal. Each spectra was normalized to the total emission (Figure 29). Small differences among spectra of mixtures containing more than 60% were noted. The mixture THF/H₂O 50/50, instead, showed a positive and more intense signal. Reasons for this behaviour are still not clear but this system probably deserves to be investigated further.

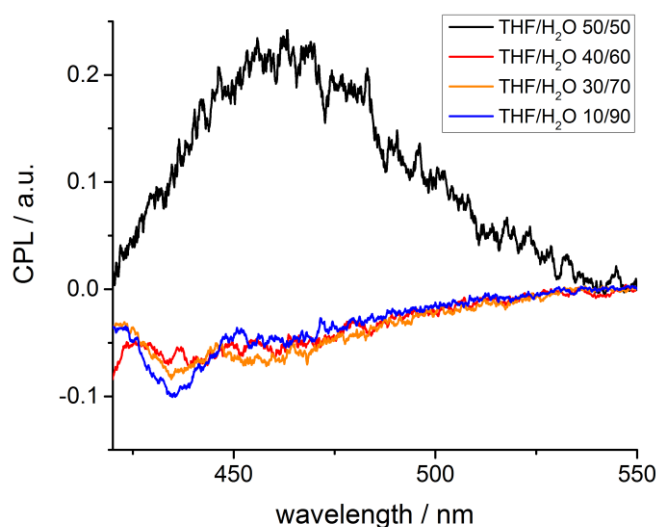


Figure 29. CPL spectra of compound **2** in different mixtures THF/H₂O, concentration $5 \cdot 10^{-5}$ M, RT.

2.3.2 Solid state characterization

The chiroptical properties of the synthesised compounds were assessed for samples in different forms: as powder, thin film or crystals.

Few milligrams of compound **2** were finely dispersed in mineral oil (Nujol) and two drops of this dispersion were pressed between two quartz slides. CD and absorption spectra recorded after that, are shown in Figure 30. Samples were also analysed rotating the slide by 90° around the optical axis to assess homogeneity of the sample and detect possible linear dichroism effects.

A positive Cotton effect for band I and a weak positive couplet for band II were observed. The CD spectra indicated that there is some kind of helical order also in the powder, but the structure is probably different from the aggregates in solution. Compound **2** as powder, exhibited also visible blue emission (Figure 31) and was therefore analysed by CPL and fluorescence spectroscopy. The emission spectra showed an emission band with λ_{max} 440 nm, slightly blue-shifted compared with spectra in THF/H₂O mixtures. A negative CPL band associated to this band was also observed. In this case, the negative sign is not in agreement with the positive lower-wavelengths CD band, but we found no trivial explanation for this behaviour.

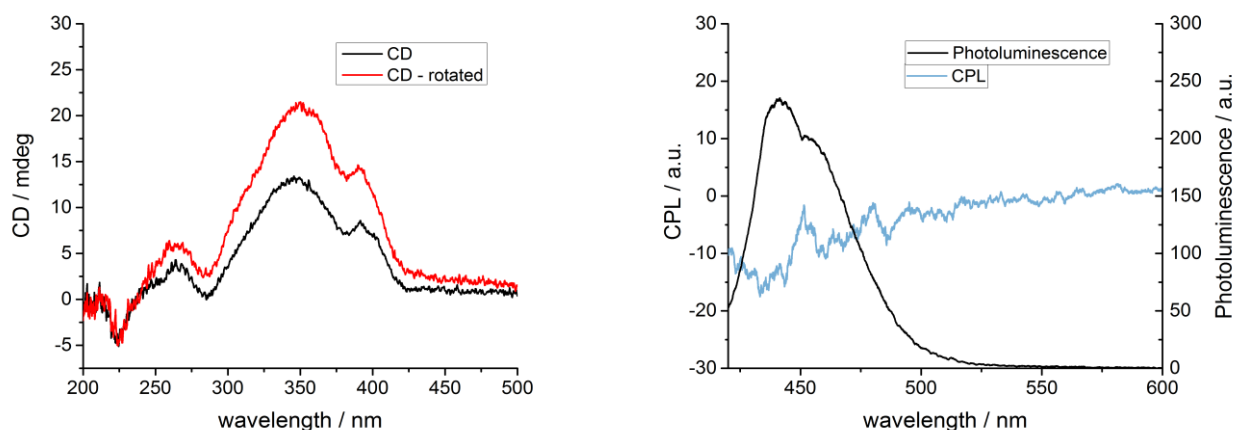


Figure 30. CD spectra of Nujol dispersion of compound **2** as powder. Two measurements shown were performed rotating the slide by 90 degrees around the optical axis (left). CPL and emission spectra of Nujol dispersion of compound **2** as powder (right).

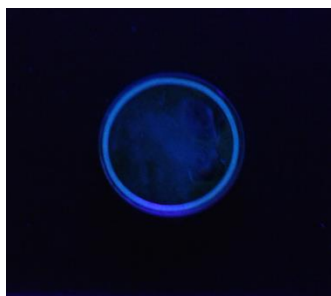


Figure 31. Photo of compound **2** as powder dispersed in Nujol, under 365 nm UV-lamp irradiation.

Crystals of **2** in form of small needles, were grown by vapor diffusion of pentane into a chloroform solution of **2**, obtaining small light-green needles. Information about the crystalline geometry packing was given us by X-ray analysis. The monoclinic unit cell was assigned to the $P2_1$ enantiomorphic space group. The unit cell had a long axis along the direction perpendicular to the π - π stacking. No helical arrangements along the stacking direction was observed but the naphthalene diimide chromophores planes were found parallel to each other, and the distance between them (3.33\AA) was consistent with aromatic face-to-face interactions. The aromatic centres were offset both longitudinally and in the transverse direction and thus there was only partial overlap of the aromatic faces. The unit cell is organized in different piles, within which naphthalene diimides chromophores resulted parallels to each other, giving a non-chiral arrangement. However, different piles were found tilted with respect to each other creating a chiral environment. Therefore, only a weak exciton couplet could be hypothesized in CD spectra, due to possible inter-piles coupling (Figure 32).

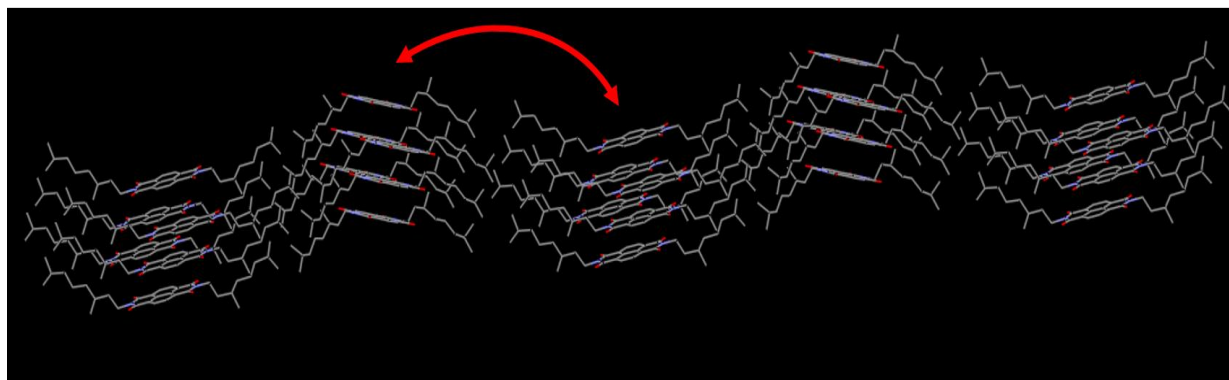


Figure 32. Unit cell of compound **2**. Arrow indicates possible exciton coupling between chromophores in different piles.

The crystals were analysed via chiroptical spectroscopy employing two different methods. In the first method, the crystals were smashed, dispersed in mineral oil (Nujol), and pressed between two quartz glasses. CD and CPL spectra were recorded and are shown in Figure 33. CD spectrum showed band pattern similar to the spectrum of the same compound as a powder. The crystals exhibited also the negative CPL band in correspondence of the blue emission typical of this compound in aggregate form.

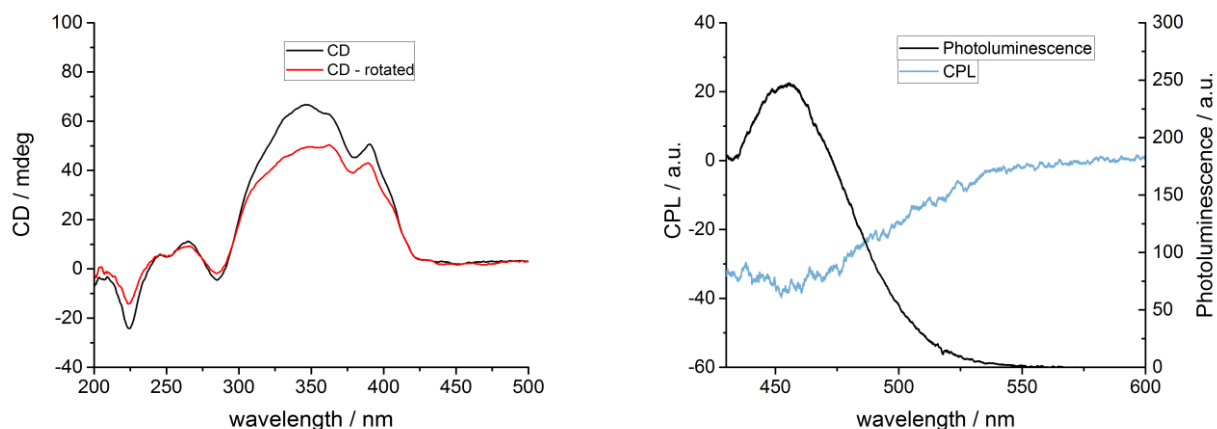


Figure 33. CD spectra of Nujol dispersion of compound **2** in crystalline form. Two measurements shown were performed rotating the slide by 90 degrees around the optical axis (left). CPL and emission spectra of Nujol dispersion of compound **2** as powder (right).

Absorption Anisotropy factor g was calculated for both powder and crystals sample and plotted as function of wavelength in the range of interest (Figure 34). About 3 times higher absolute values could be observed for crystals, in particular for band I, with best value around 0.015 at 350 nm. These data suggested that in crystals and powder, molecules are arranged with the same chirality. Nevertheless, the powder contains both amorphous and crystalline domains.

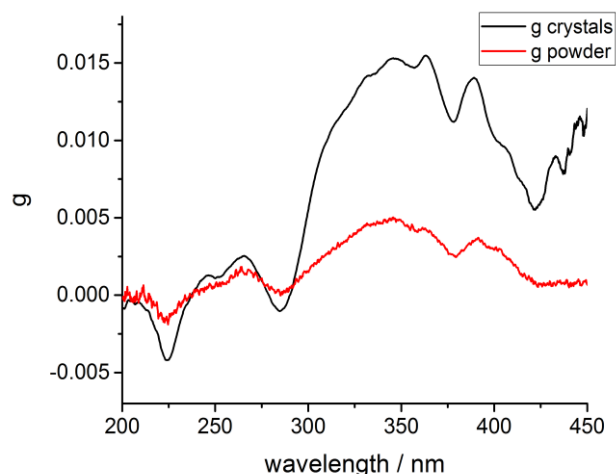


Figure 34. Plot of anisotropy factor g against wavelength for compound **2** as crystals and as powder.

In the second method, the crystals were finely dispersed in dry KCl and pressed to obtain a disk. CD spectrum of the KCl disk was then recorded, to assess differences compared to the sample dispersed in Nujol. In this case, the spectrum looked very different. Both bands I and II revealed a weak negative couplet, in contrast with positive band in the range 300-400 nm previously observed. This spectrum could be in agreement with the crystalline packing observed by X-ray diffraction analysis. The differences in behaviour between the two methods, could be given admitting that preparation with Nujol, even not dissolving the sample, induced some rearrangements in the crystalline structure. On the other hand, high pressure were employed to obtain the KCl disk, possibly modifying the original crystalline structure.

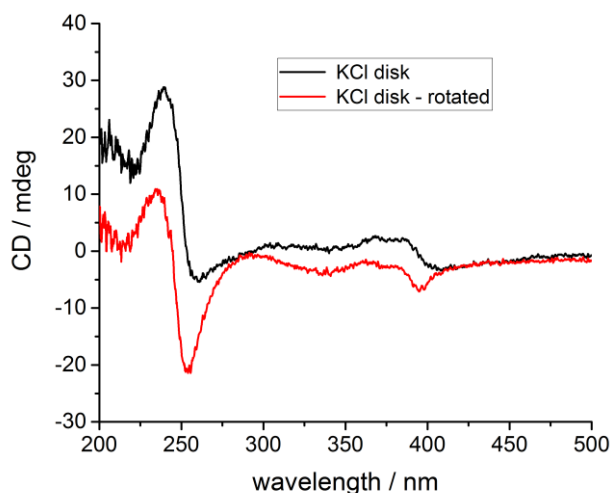


Figure 35. CD spectra of KCl disk of compound **2** in crystalline form. Two measurements shown were performed rotating the slide by 90 degrees around the optical axis.

Thin films characterization

There are currently several techniques which allow to deposit solutions on surfaces to obtain thin films (Spin-coating, Langmuir-Blodgett, Chemical Vapor Deposition). In electronic devices production it is an important issue because properties of materials can strongly vary depending on the chosen technique. The most common techniques performed in lab are probably drop-casting and spin-coating. Spin-coating allows one to prepare thin film with good homogeneity and definite thickness. On the other hand, a solvent which completely dissolves the compound is needed. Moreover evaporation of the solvent during the spinning is almost instantaneous, preventing in some cases reorganization of molecules in most stable structures. In some cases, it is also possible to obtain amorphous or partially crystalline films depending on the spin rate.

10 mg/ml chloroform solution of **2** was prepared and few drops were spincoated at 2000 rpm on a glass surface. Thin film obtained resulted in an almost transparent and amorphous film as confirmed by POM. Film was then subjected to thermal annealing at 100°C for 2 hours. Partial crystallinity was observed after annealing by POM as result of reorganization of molecules in more stable supramolecular structures (Figure 36).

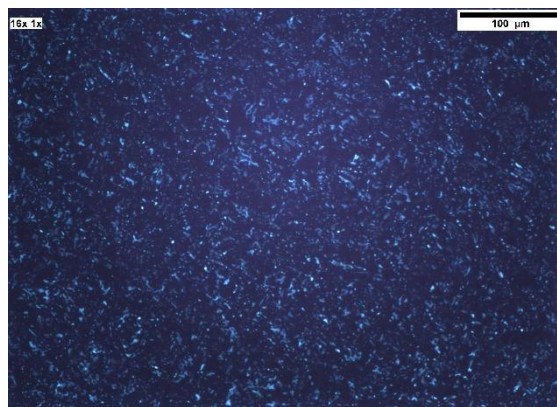


Figure 36. POM view of thin film of compound **2** after annealing 2 hours at 100 °C.

Thin film sample was measured by CD spectroscopy before and after annealing. CD spectra confirmed that very weakly ordered aggregates were present in the amorphous film, but after annealing treatment the order successfully increased (Figure 37). The Cotton effect was much more intense after annealing, and the sign of the band at 400 nm was inverted. Two aggregates of opposite helicity may be involved in this effect. The high anisotropy factor g at 400 nm (average value of two measurements is around +0.05) confirmed that high order in solid can be reached in suitable conditions. In this case, when the temperature is high enough the aggregates in amorphous phase can acquire sufficient energy to reorganize in more thermodynamically stable aggregates.

Drop-casting technique is appealing for its simplicity and for slow evaporation which can help intermolecular reorganization. Drawbacks are difficulty in control of homogeneity and thickness of the film. The same solution (10 mg/ml in chloroform) used for spin-coating was drop-casted on a quartz glass and after spontaneous evaporation of the solvent, CD spectrum was recorded (Figure 37). A positive Cotton effect was observed for band I, similarly to the cases of the spin-coated film after annealing, of the powder and crystals. The band was also more intense than in previous cases, due to the more thick layer of sample obtained by drop-casting technique with concentrate solutions. Cotton effect at lower-wavelengths was instead slightly different in shape, compared with spectra of the powder already discussed, but we did not find an explanation for this difference. Smaller linear dichroism effects were observed for the drop-casted film. Absorption anisotropy factor g was calculated also for all the film described. g values as -0.07 and 0.11 could be reached at 250 nm and 350 nm respectively by simple dropcast. These high values, suggested that this compound could efficiently discriminate the handedness of the circularly polarized light, in an OFET-based sensor for example.

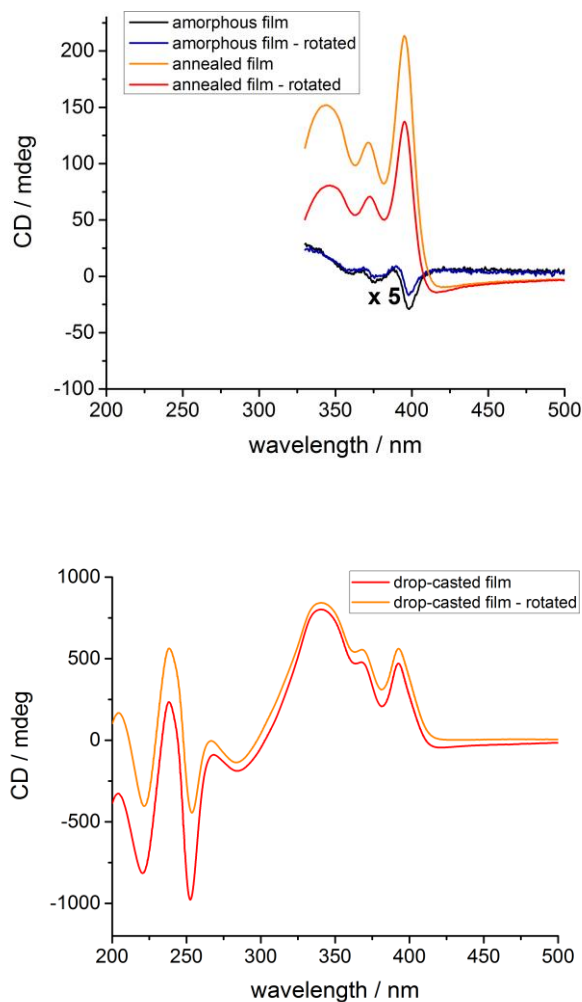


Figure 37. Comparison between CD spectra of thin films obtained by spin-coating and drop-casting. CD spectra of compound **2** as thin film obtained by spin-coating at 2000 rpm of 10 mg/ml solution in chloroform, before and after annealing; amorphous film is multiplied by 5 to make it visible in the scale used. The spectra could not be registered below 330 nm due to glass absorption (top). CD spectra of compound **2** as thin film obtained by drop-casting of 10 mg/ml solution in chloroform (bottom). Two measurements for each sample were performed rotating the slides by 90 degrees around the optical axis.

2.4 Characterization of the Carboxylic Acid appended Naphthalene Diimide

2.4.1 Optical and chiroptical characterization in solution

In this chapter the aggregation properties of compound **3** will be discussed (Figure 38).

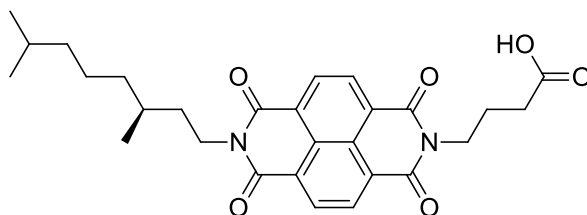


Figure 38. Structure of the chiral carboxylic acid appended NDI **3**

In particular, we wanted to investigate the role of hydrogen bonding in self-assembly,⁸⁰ compared to compound **2** analysed in the previous chapter. UV-Vis spectra were first recorded in a good solvent (chloroform or 1,1,2,2-tetrachloroethane) with increasing percentage of bad solvent (cyclohexane or methylcyclohexane). Solutions were prepared adding the required volume of bad solvent to solutions of **3** in the good solvent in order to obtain $5 \cdot 10^{-5}$ M concentration. When at least 90 % of MCH was added, the absorption spectra showed the rising of a new red-shifted peak at 396 nm for band I, with the simultaneous decrease of the monomer band (Figure 39).

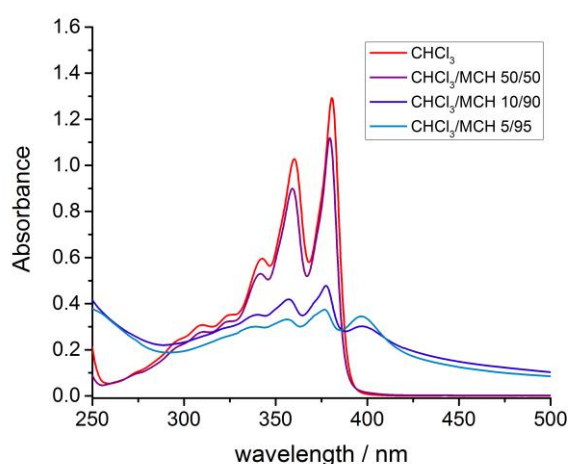


Figure 39. UV-Vis spectrum of compound **3** in in different mixtures CHCl_3/MCH , concentration $5 \cdot 10^{-5}$ M, RT (left).

⁸⁰ M. R. Molla, S. Ghosh, *Chem. Eur. J.*, **2012**, *18*, 1290-1294

No significant red-shift could be observed for band II. The spectrum exhibited scattering due to scarce solubility of the acid-appended NDI **3** in the mixture. In order to investigate the aggregation on variable temperature we measured UV-Vis spectra of **3** between 85 °C and 5 °C every 10 K at $5 \cdot 10^{-5}$ M. To this end we switched from CHCl_3 to the higher boiling TCE, which is also a good solvent. A solvent mixture of TCE/MCH 5/95 was used, since we knew that aggregates are formed at room temperature in these conditions.

We started from 85 °C making sure that the solution was composed only by monomers in order to follow the aggregation process. We waited 10 minutes between a measurement and the next one. Above 45 °C the absorption spectrum looks similar to the one previously recorded in chloroform at room temperature, indicating that only monomeric species exist above this temperature. At lower temperature, the intensity of the monomer band decreases and the new peak with λ_{max} at 396 nm can be seen (Figure 40). Therefore, the critical temperature for the aggregation process was found around 45 °C. Small changes in the spectrum could also be seen for band II at 260 nm. The peak at 396 nm resulted quite weak compared to the spectrum of the mixture CHCl_3/MCH shown in Figure 39, probably due to precipitation of macroaggregates under cooling.

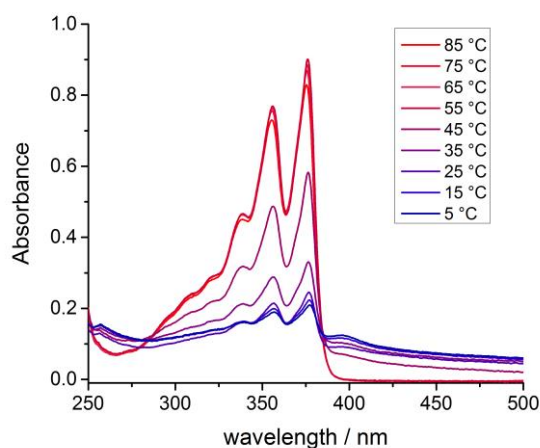


Figure 40. UV-Vis spectrum of compound **3** in TCE/MCH 5/95 at variable temperature, concentration $5 \cdot 10^{-5}$ M .

Emission properties of **3** under aggregation were also investigated. Carboxylic acid-appended naphthalene diimides in aggregate form were already known in literature for their interesting photoluminescence properties.⁴⁶ Emission spectra of **3** were recorded in the same solvent mixture TCE/MCH 5/95 already used for UV-Vis measurements. The spectra were recorded exciting the 0-1' peak of band I vibronic progression at 356 nm. To disassemble any kind of aggregate, the solution was kept 30 minutes at 85 °C before starting the measurements. Then, the spectra were recorded every 10 K until -5 °C (shown in Figure 41). Above 55 °C the emission spectrum was structured and

resemble the mirror-image of the absorption spectrum in chloroform (Figure 39), indicating that the acid **3** is in its molecularly dissolved state (monomer emission). The 0'-0 band was less intense because of self-absorption effect. At 45 °C the monomer emission became less intense and a new band in the range 450-650 nm arose. White-yellow emission from aggregate species was visible (Figure 41).

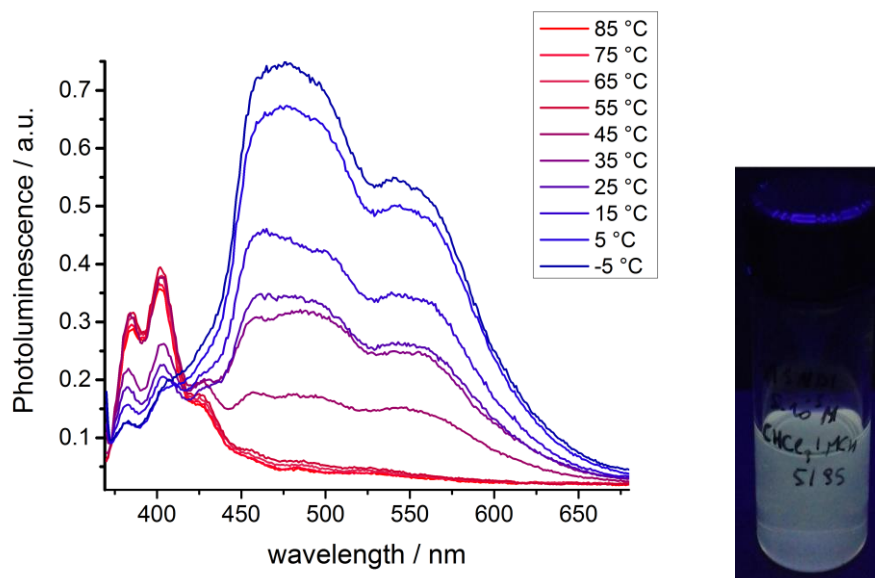


Figure 41. Emission spectra of compound **3** in TCE/MCH 5/95 at variable temperature, excitation wavelength 356 nm, concentration $5 \cdot 10^{-5}$ M (left). Photo of **3** in CHCl_3/MCH 5/95 under UV lamp irradiation, RT (right).

As in similar cases, broad and unstructured emission band could suggest the formation of excimer species induced by ground state aggregation.⁸¹ Multiple aggregates species could contribute to emission in different zones of the band, giving as result yellow-white light.

To investigate supramolecular order of compound **3**, circular dichroism and circularly polarized luminescence experiments were carried out on solution $\text{CHCl}_3/\text{Cyclohexane}$ 5/95, $5 \cdot 10^{-5}$ M. The spectrum showed intense negative cotton effects for both short and long-axis polarized electronic $\pi-\pi^*$ transition. The negative exciton couplet in the range 300-400 nm reflected the vibronic structure of band I in absorption. The high-energy Cotton effect was partially not visible because of the solvent cut-off. However, the negative band observed at 256 nm may be assigned to the negative part of a bisignate exciton couplet, in comparison with solid state spectra reported further.

⁸¹ T. D. M. Bell, S. V. Bhosale, C. M. Forsyth, D. Hayne, K. P. Ghiggino, J. A. Hutchison, C. H. Jani, S. J. Langford, M. A.-P. Leea. C. P. Woodward, *Chem. Commun.*, **2010**, 46, 4881–4883.

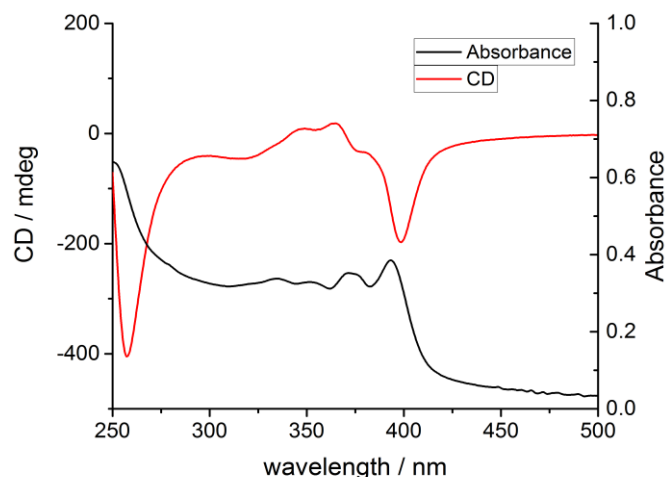


Figure 42. CD spectra of compound **3** in CHCl₃/Cyclohexane 5/95, concentration $5 \cdot 10^{-5}$ M, RT.

The values of the anisotropy factor g associated to the negative bands at 400 and 256 nm were found around -0.02 with a slightly higher absolute value for the high energy band. This order of magnitude is not so common for supramolecular aggregates. However, decreasing of CD and Absorbance signals observed after few hours, indicated that large aggregates are not thermodynamically stable in solution and tend to precipitate.

To follow the formation of aggregates and assess their stability, CD spectra were also recorded in TCE/MCH 5/95 at different temperatures under cooling. Each spectrum is collected 10 minutes after the previous one to let the aggregate reach equilibrium. Recorded CD spectra are shown in Figure 43. The CD spectrum is silent above 45 °C. Below that critical temperature, Cotton effects for both band I and II can be observed. However, compared with the spectrum at room temperature of the freshly prepared solution, two differences could be noted: the CD signal was in general less intense, and the negative band at 405 resulted more intense than negative band at 260 nm. Furthermore, strong scattering was observed since the molecules started to aggregate, suggesting again that precipitation occur over time. The negative signs of band at 260 nm and 405 nm could suggest an M-type helical rearrangement for both transition dipole moments.

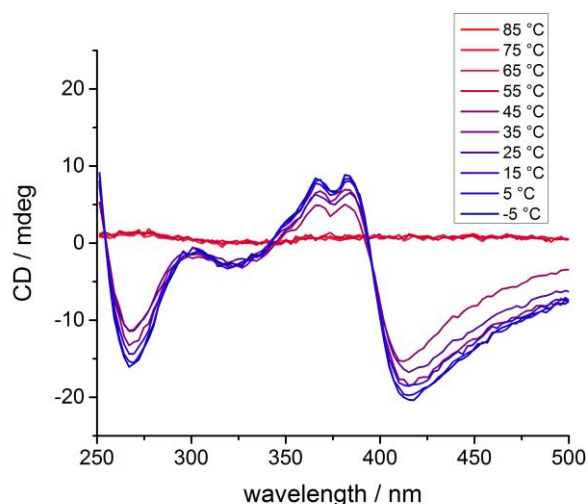


Figure 43. CD spectra of compound **3** in TCE/MCH 5/95 at variable temperature, concentration $5 \cdot 10^{-5}$ M .

A CHCl_3 /Cyclohexane 5/95 solution, $5 \cdot 10^{-5}$ M, of the acid-functionalized NDI **3** was excited with a UV lamp on the monomer band at 365 nm. CPL signal and total emission detected for the excimer band is shown in Figure 44. Two negative CPL bands could be seen in correspondence to the excimer emission. The sign of the bands (negative) was the same of the low-energy transition in the CD spectrum, indicating that handedness of excited state aggregate is the same as in the ground state aggregate.

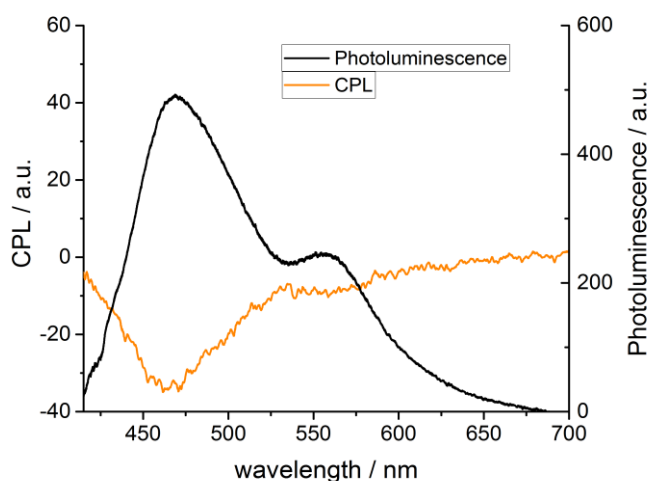


Figure 44. CPL and emission spectra of compound **3** in CHCl_3 /Cyclohexane 5/95, concentration $5 \cdot 10^{-5}$ M, RT.

As for circular dichroism, also for circularly polarized luminescence, one can define an anisotropy factor g_{lum} which quantifies the enantiomeric purity of light emission. Same order of magnitude of g

in absorption was observed. Average g_{lum} values, obtained on four measurements for lower and higher energy bands, are respectively -0.01 (550 nm) and -0.02 (450 nm). Interestingly, quite homogeneous values of g_{lum} could be obtained on the whole emission range (Figure 45).

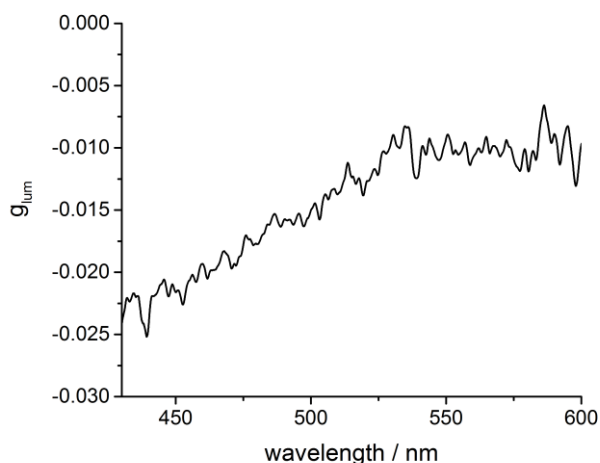


Figure 45. Plot of anisotropy factor g_{lum} against wavelength for compound **3** in $\text{CHCl}_3/\text{Cyclohexane}$ 5/95, concentration $5 \cdot 10^{-5}$ M, RT.

Variable temperature experiments

To investigate which mechanism is involved in the formation of these aggregates, Absorption and CD signals of the compound **3** at specific wavelengths were recorded during cooling-heating cycles. Starting from 80 °C, the solution was cooled at rate of 60 °C/h, and the absorbance was followed at two different wavelengths: 376 nm and 396 nm. These are the 0-0' monomer band and aggregation peak maxima, respectively. In this way, we followed the monomer disappearance and the formation of the aggregates at the same time. After the first cycle, the solution was kept 5 minutes at 80 °C and a second cycle in the same conditions was performed. As shown in Figure 46 cooling curves are clearly non-sigmoidal, indicating a cooperative mechanism (see paragraph 1.2). Critical temperature for the elongation process was found around 45°C coherently with spectra reported in the previous paragraph. A certain amount of hysteresis can also be noted. When the experiment was carried out at lower rate (15 °C/h) from 85 °C to -5 °C, the 396 nm peak at the plateau was less intense than in higher cooling rate case. This effect could be also due to precipitation of macroaggregates during the cooling process, that was more important when lower cooling/heating rate was involved.

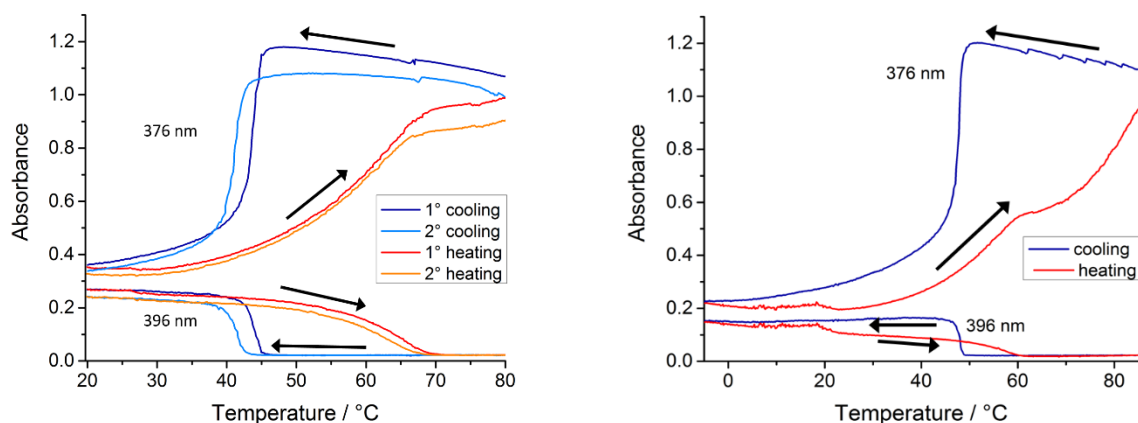


Figure 46. Plot of Absorbance in function of temperature at 376 and 396 nm under cooling/heating cycle. Rate 60°C/h (left), 15°C/h (right).

We also followed the formation of the aggregates by CD at 405 nm, in correspondence of the higher-wavelengths negative band. The same mixture TCE/MCH 5/95 was used, starting from 80 °C with 60 °C/h rate (Figure 47).

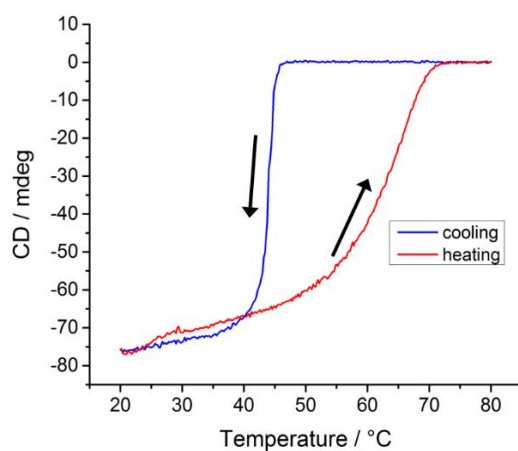


Figure 47. Plot of CD in function of temperature at 405 nm under cooling/heating cycle rate 60 °C/h.

Also in this case, a non-sigmoidal curve was obtained, confirming a cooperative aggregation mechanism. Critical temperature value was consistent with absorption experiments.

2.4.2 Solid state characterization

The chiroptical properties in solid state, were assessed for the compound **3** as powder and thin film. Few milligrams of compound **3** as powder were finely grinded and dispersed in mineral oil (Nujol) and two drops of this dispersion were pressed between two quartz slides. CD and CPL spectra recorded are shown in Figure 48. The CD spectrum showed a vibronic structured negative exciton couplet for band I around 400 nm, similarly to aggregates obtained in the mixture TCE/MCH 5/95. However band II at 250 nm showed a positive exciton couplet in contrast with previous solution spectra. Circularly Polarized Luminescence spectra were also recorded. The CPL spectra showed the same excimer-like band found in the mixture TCE/MCH 5/95, with good g_{lum} value of -0.01 around 450 nm.

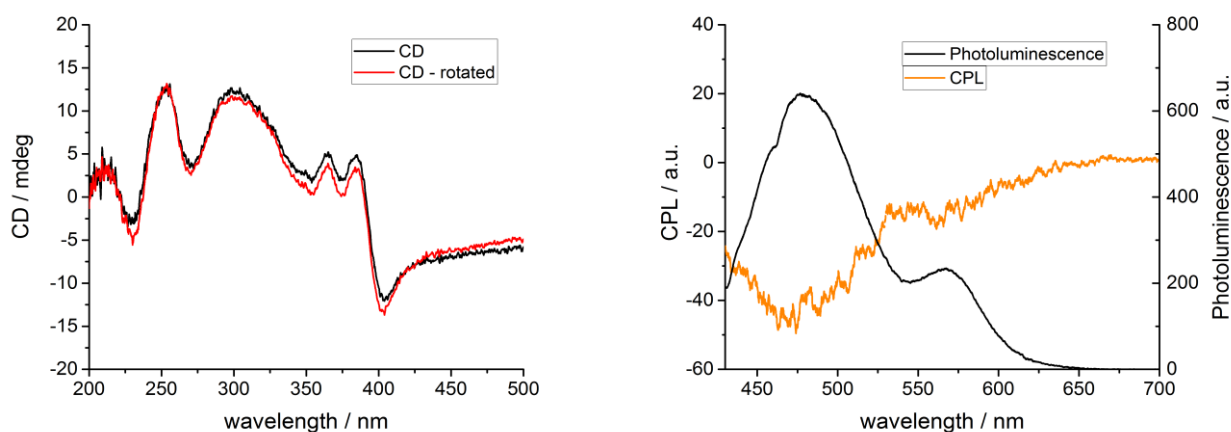


Figure 48. CD spectra of Nujol dispersion of compound **3** as powder. The two measurements shown were performed rotating the slide by 90 degrees around the optical axis (left). CPL and emission spectra of Nujol dispersion of compound **3** as powder (right).

Solid samples exhibited visible yellow-white fluorescence under UV-lamp irradiation as can be seen in Figure 49.

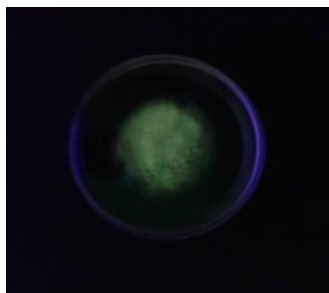


Figure 49. Photo of dispersion in Nujol of compound **3** as powder, under 365 nm UV-lamp irradiation.

Thin films characterization

Most of electronic applications require easy processability and homogeneous properties of the materials, usually in the form of thin films. Accordingly, we aim to investigate properties of compound **3** as thin film. To this end, 10 mg/ml chloroform solution of the acid appended NDI was prepared and few drops were spin-coated at 2000 rpm for 60 seconds on a glass surface. The thin film obtained resulted in an almost transparent and amorphous film as confirmed by POM analysis. It was then annealed at 100 °C for 2 hours. CD spectra were recorded before and after annealing. The glass slide was analysed in different zones rotating the sample by 90° around the excitation light axis to assess homogeneity of the sample and detect linear dichroism effect. Only negligible CD signal could be detected in amorphous film. After annealing instead, a negative exciton couplet was observed for band I. However, the weak signal suggested that mobility of **3** in solid state is not as high as for **2**, probably because of hydrogen bonding interactions which slow down possible rearrangements. Long tail on the low-energy side of the spectrum arose from scattering due to inhomogeneity of the film.

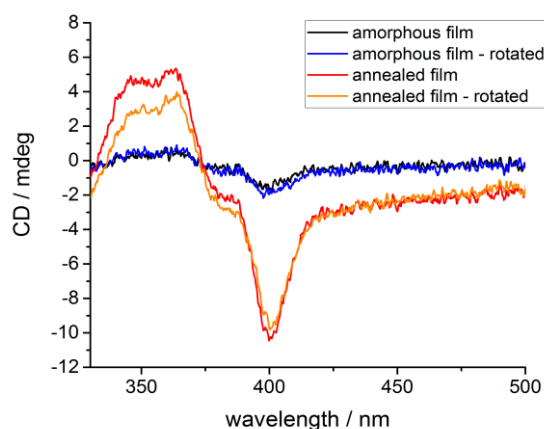


Figure 50. CD spectra of compound **3** as thin film obtained by spin-coating at 2000 rpm of 10 mg/ml solution in chloroform, before and after annealing. The two measurements shown were performed rotating the slide by 90 degrees around the optical axis.

To investigate whether supramolecular chirality was transferred from solution to solid state, the same solution CHCl₃/Cyclohexane 5/95 of **3** ($5 \cdot 10^{-5}$ M) already used (see Figure 42), was drop-casted on a quartz glass. After spontaneous evaporation of solvent, thin film obtained was studied by CD spectroscopy (Figure 51).

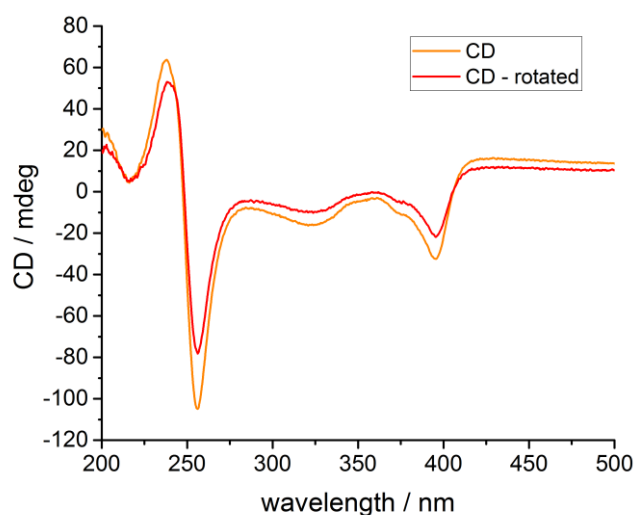


Figure 51. CD spectra of compound **3** as thin film obtained by drop-casting of CHCl₃/Cyclohexane 5/95, concentration 5·10⁻⁵ M. The two measurements shown were performed rotating the slide by 90 degrees around the optical axis.

CD spectra showed again two negative exciton couplets for both band I and II. The shape of the spectrum was preserved indicating similar order in the aggregates even after solvent evaporation. A scattering component due to film inhomogeneity was observed in the low-energy side of the spectrum. High *g* values were obtained also in this case (around -0.045 at 256 nm and -0.02 at 400 nm, average values). Unfortunately, emission of thin film obtained by drop-casting was not intense enough to be recorded by our CPL instrument.

2.5 Characterization of the Amide Appended Naphthalene Diimide

2.5.1 Optical and chiroptical characterization in solution

Compound **5** (Figure 52) allowed us to investigate differences in hydrogen-bonding behaviour between the amide and the carboxylic acid group.

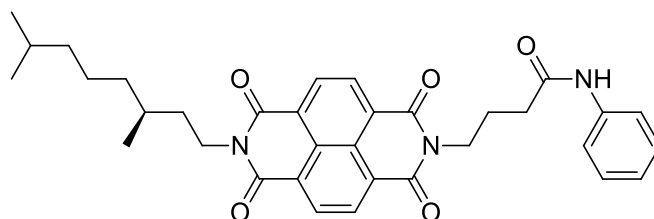


Figure 52. Structure of the chiral NDI **5** functionalized with an amide group.

UV-Vis experiments were carried out first. To trigger self-assembly in solution, mixtures of TCE with increasing amount of MCH as bad solvent were tried. Solvents as toluene or THF were also tested but no aggregation was observed in any case. Absorption spectra were recorded for solutions $5 \cdot 10^{-5}$ M. However no changes in the spectrum were observed even for 95% of MCH compared with molecularly dissolved situation in TCE (Figure 53). The hypsochromic shift observed was due to diminished polarity of the solvent mixture. Thus we tried to induce aggregation in pure MCH recording spectra at different temperatures under cooling starting from 85 °C (Figure 53). While the monomer band shape remained unmodified, the intensity strongly decreased. Below 35 °C, the spectrum showed scattering and below 15 °C the new peak at 396 nm indicative of aggregation was observed. At the same time even more intense scattering was visible probably due to precipitation of **5**.

Fluorescence spectra of compound **5** in MCH were also recorded at different temperature, cooling the solution from 65 °C to 5 °C (Figure 54). Weak signal was observed for the whole emission. A very small decrease of the intensity of the peaks at 400 and 425 nm, along with an increase of the band at 500 nm was detected. In this case, compared with the emission spectra of compound **2**, we could not attribute this changes to excimer species, since the absorption spectra already showed a small evolution in the same conditions.

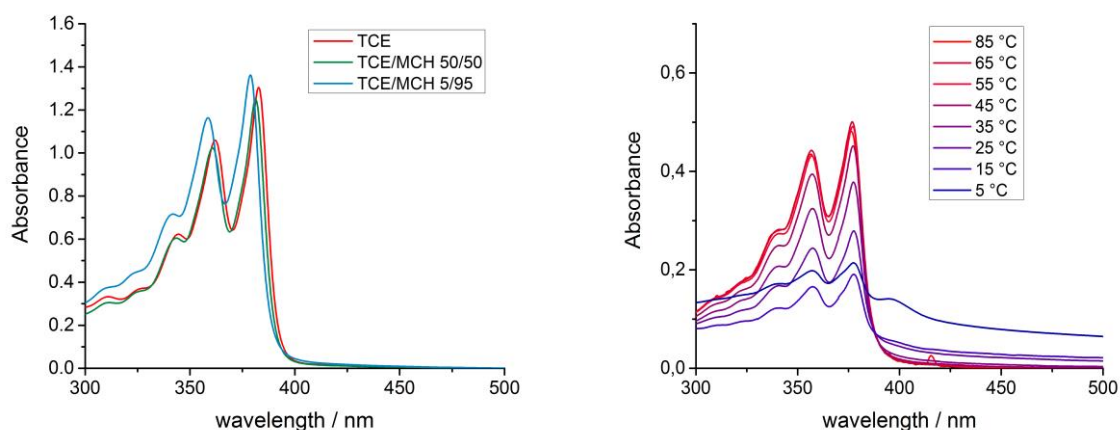


Figure 53. UV-Vis spectrum of compound **5** in different mixtures TCE/MCH at RT (left), and in MCH at variable temperature (right). Concentration $5 \cdot 10^{-5} \text{M}$.

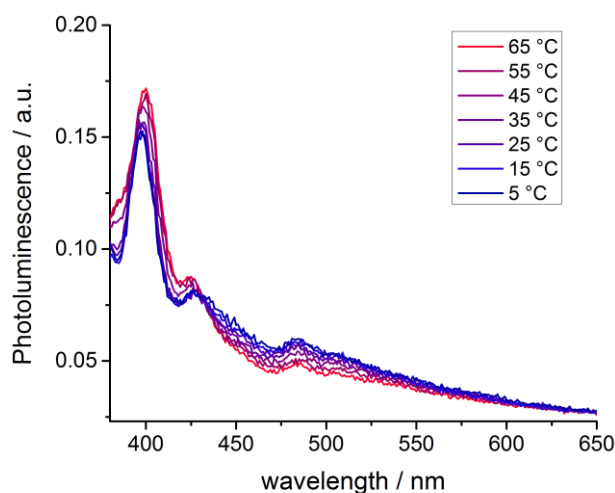


Figure 54. Emission spectra of compound **2** in MCH at variable temperature, concentration $5 \cdot 10^{-5} \text{M}$.

CD spectroscopy was performed on MCH solution of **5** to collect more information about this less pronounced tendency to aggregation. Starting from 85 °C, CD spectra were recorded every 10 K, and the solution was allowed to equilibrate 10 minutes before each measurement (Figure 55). Below 35 °C, the spectra showed a weak negative band at 400 nm and a positive band at 260 nm. The signal was anyway very noisy, but no effect due to scattering was observed.

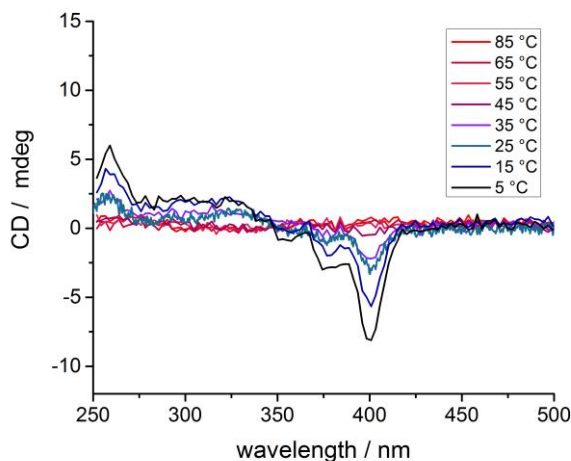


Figure 55. CD spectra of compound **3** in TCE/MCH 5/95 at variable temperature, concentration $5 \cdot 10^{-5}$ M.

2.5.2 Solid state characterization

A 10 mg/ml chloroform solution of **5** was prepared and few drops were spincoated at 2000 rpm for 60 seconds on a glass surface. POM analysis confirmed that thin film obtained were completely amorphous. The film was then annealed at 100 °C for 2 hours. CD spectra were recorded before and after annealing and are shown in Figure 56. Only negligible CD signal was observed in amorphous film, and after annealing a very small change could be detected. Several works in literature exploit amide hydrogen bonding in combination with π -stacking to obtain supramolecular structures. However, compound **5** did show a very weak tendency to aggregation both in solution and solid state. There could be several reasons for this poor behaviour. Probably, the C_3 -spacer between naphthalimide and amide functionalities and the rigidity of phenyl moiety bonded to amide nitrogen prevent in some way a favourable intermolecular H-bonding array. Compound **5** was not investigated further.

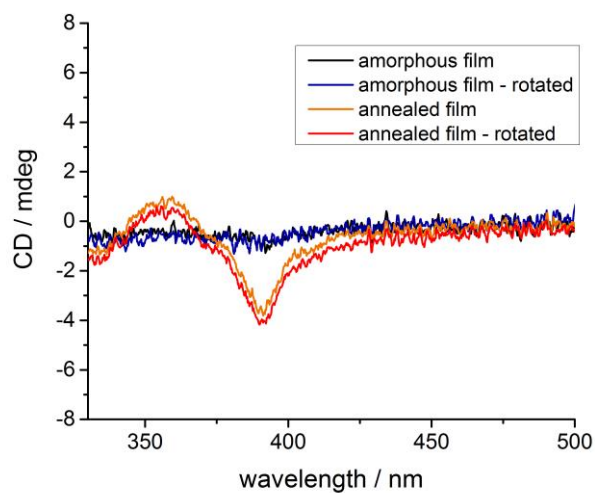


Figure 56. CD spectra of compound **5** as thin film obtained by spin-coating at 2000 rpm of 10 mg/ml solution in chloroform, before and after annealing. The two measurements shown were performed rotating the slide by 90 degrees around the optical axis.

Conclusion and Outlook

In this work three new chiral naphthalene diimide derivatives **2**, **3** and **5** bearing different functional groups were synthesised and characterized by standard organic analysis. Their self-assembly properties were studied in solution upon the addition of a suitable bad solvent and in solid state as well via chiroptical spectroscopy. Differences among the three NDI derivatives and for different conditions were highlighted.

Even though several supramolecular architectures bearing amide functionality are known in literature, in molecule **5**, the amide group was not able to promote a stable H-bonding network in hydrocarbon solvent. Considering that many molecules designed for self-assembly bear no less than two amide groups, a single amide group per molecule is probably insufficient to promote aggregation. As we observed, the same is not true for molecules containing more polar functionalities as compound **3**, where a single carboxylic group determine the aggregation in hydrocarbon solvents. In this case a completely apolar solvent does not interfere with H-bonding networks but encourage it, solvating the lipophilic part of the aggregate. The acid-appended naphthalene diimide **3** formed supramolecular structures with interesting emission properties: white-yellow emission both in solution (when 95% of MCH or cyclohexane is in the mixture) and in solid state. High anisotropy factors (in the range -0.01/-0.02) both in absorption and in emission were observed on the whole range of interest. This emission properties could be in future exploited for an NDI-based Circularly Polarized OLED.

On the other hand, polar solvents were efficient to trigger the aggregation of compound **2**, promoting attractive interaction between alkyl chains. Aggregates were detected in THF solution when at least 50% volume of water was added. Ordered aggregates with different geometries can be probably formed also in solid state. CD spectroscopy showed that different aggregation modes are possible depending on the preparation of the sample. Unusually high absorption anisotropy factors have been detected in solid state, in particular in thin films, obtained from drop-casting of a concentrated CHCl_3 solution (around +0.1), which make this compound a good candidate for the realization of an OFET sensitive to handedness of the circularly polarized light.

In solid state, we observed a higher flexibility of the system **2**, which can undergo different and big modifications when subjected to thermal annealing, slow evaporation or crystallization process. In favourable conditions (in solution or high temperature), the alkyl chains can probably slide on each other until a favourable supramolecular structure is reached. When the NDI derivative contains a carboxylic or amide group instead, rearrangement resulted slower. A slight better cooperativeness of carboxylic groups compared with amide groups was observed from CD characterization of thin films.

Further investigations on the structure of the aggregates in solution formed by NDIs **2** and **3** have to be performed. Moreover, a deeper understanding of their properties in solid state will be essential in order to apply these molecules in organic electronic devices.

3 Experimental Section

3.1 Materials and methods

- All starting materials were obtained from commercial suppliers and used as received. All moisture-sensitive reactions were performed under an atmosphere of dry argon. Dry dichloromethane were obtained by distillation from P₂O₅, and triethylamine was dried over potassium hydroxide. N-methyl pyrrolidone was kept under molecular sieves 4Å overnight before use.
- Column chromatography was performed on a Biotage Isolera One using KP-SNAP columns and solvent gradients.
- Microwave reactions were performed on a Biotage Initiator reactor. All the reactions were performed with power set to 300 W.
- ¹H NMR and ¹³C NMR spectra were recorded on a 400 MHz 4-nucleus NMR (Varian Mercury Vx) (400 MHz for ¹H NMR and 100 MHz for ¹³C NMR). Proton and carbon chemical shifts are reported in ppm downfield from tetramethylsilane (TMS) using the resonance of the deuterated solvent as internal standard.
- Matrix-assisted laser desorption/ionization mass spectra were obtained using α-Cyano-4-hydroxycinnamic acid (CHCA) and *trans*-2-[3-(4-*tert*-Butylphenyl)-2-methyl-2-propenylidene]malononitrile (DCTB) as matrices on a PerSeptive Biosystems Voyager-DE PRO spectrometer.
- IR spectra were measured on a Perkin-Elmer 1600 FT-IR.
- DSC spectra were obtained on a Perkin-Elmer Pyris 1 DSC.
- Polarisation Optical Microscopy (POM) measurements were performed on a Jenaval polarisation microscope equipped with a Linkam THMS 600 heating device, with crossed polarizers.
- Single-crystal X-ray diffraction studies were performed on a Nonius Kappa CCD Single-crystal X-ray diffractometer.

- GPC measurements were carried out using a column with PL gel and chloroform as eluent and a flow rate of 1 mL min⁻¹; detection was carried out on a UV detector at a wavelength of 254 nm.
- Circular dichroism (CD) spectra were measured using a J-710 CD spectrometer. Temperature dependent CD measurement were performed on a Jasco J-815 with temperature controlled by a PTC-348WI Peltier system. Ultraviolet-visible (UV-Vis) absorbance spectra were recorded using a Jasco V-650 UV-Vis spectrometer with a Jasco ETCT-762 temperature controller. Fluorescence emission spectra were recorded on a Fluorolog Horiba Jobin-Yvon. The path length of the cuvettes was 1 cm for all the measurements.
- Circularly Polarized Luminescence (CPL) spectra were measured using a home-made instrument, using 365 nm excitation UV-lamp. The instrument was built using the chassis, photoelastic modulator (PEM), lock-in amplifier and photomultiplier tube of a decommissioned Jasco J-500 C spectropolarimeter. The PEM, followed by a linear polarizer, is placed in front of the sample holder. The light then passes through a Jasco CT-10 monochromator (1200 grooves/mm blazed at 500 nm) driven by a step motor controlled by an electronic prototyping platform. The same platform digitalizes the analog output signals (both direct and alternate current signals). The spectra are plotted in real time in an Excel spreadsheet.

3.2 Synthetic Procedures

3.2.1 Synthesis of NMI 1 and NDI 2

1,4,5,8-Naphthalene tetracarboxylic dianhydride (1 eq, 735 mg, 2.73 mmol) and (S)-3,7-dimethyl octylamine (1 eq, 430 mg) were added in a 20 mL microwave reaction vessel. A magnetic stirrer and DMF (10 mL) were added. The glass tube was sonicated two minutes. The reaction was carried out in two steps: 5 minutes at 75 °C and 20 minutes at 140 °C (power 300 W). The reaction mixture was then transferred in a flask, washing the tube with dichloromethane. The solvent was removed under reduced pressure to give a brown residue. NaOH_(aq) 1 M was added to the residue, and after sonication, the insoluble residue was filtered.

- 1) The solid was washed with water, then dried overnight in vacuo at 60 °C and purified by chromatography (silica gel, eluent CH₂Cl₂) to obtain 164 mg of compound **2** (yield 11%, off-white powder).
- 2) The filtrate was acidified with HCl_(aq) 3M until pH 5. The acidic mixture was filtered and the brown solid was dried overnight in vacuo at 60 °C. 522 mg of compound **1** were obtained (47% yield). The NMI **1** obtained was used directly in the next step without purification.

NMI 1

¹H-NMR (200 MHz, DMSO-d₆) δ (ppm): 8.42-7.95 (dd, 4H; naphthalene core), 4.00-4.06 (m, 4H; NCH₂), 1.11-1.56 (m, 10H), 0.94 (d, 3H; CH₃), 0.81 (d, 6H; C(CH₃)₂).

NDI 2

¹H-NMR (400 MHz, CDCl₃) δ (ppm): 8.74 (s, 4H; naphthalene), 4.17-4.24 (m, 4H; NCH₂), 1.69-1.78 (m, 2H; NCH₂CH₂CH), 1.47-1.60 (m, 6H; NCH₂CH₂, CH), 1.14-1.38 (m, 12H), 1.02 (d, 3H; CH₃), 0.85 (d, 6H; C(CH₃)₂).

¹³C-NMR (400 MHz, CDCl₃) δ (ppm): 162.73, 130.86, 126.62, 39.41, 39.23, 37.06, 34.98, 31.22, 27.91, 24.59, 22.67, 22.60, 19.53.

MS (MALDI-TOF, negative mode): m/z 546.35 (calculated), 546.38 (experimental).

FT-IR (powder) wavenumber (cm⁻¹): 1704 (m), 1656 (s), 1582 (m), 1342 (m), 1242 (m), 769 (s).

3.2.2 Synthesis of acid appended NDI **3**

The 4-aminobutyric acid (3 eq, 340 mg) and triethylamine (3 eq, 460 μ L) were added in a 20 mL glass tube for microwave reaction. DMF (20 mL) was added and the mixture was stirred 10 minutes. Then, the NMI **1** (1eq, 466 mg, 1.1 mmol) was added. The glass tube was sonicated two minutes. After that, the reaction was carried out in two steps: 5 minutes at 75 °C and 20 minutes at 140 °C (power 300 W). The reaction mixture was then transferred in a flask washing the tube with dichloromethane. The solvents were evaporated and distilled water was poured into the flask. The aqueous solution was filtered and the solid dried in vacuo at 60 °C. The product was purified by chromatography (silica gel, eluent $\text{CHCl}_3/\text{MeOH}$ 95/5, $R_f = 0.3$) to afford 233 mg of **3** as off-white powder (yield 43 %).

$^1\text{H-NMR}$ (200 MHz, DMSO-d_6) δ (ppm): 12.02 (s, COOH), 8.62 (s, 4H; naphthalene core), 4.08 (m, 4H; NCH_2), 2.32 (m, 2H; CH_2COOH), 1.89 (m, 2H; $\text{CH}_2\text{CH}_2\text{COOH}$), 1.12-1.60 (m, 10H) 0.96 (d, 3H; CH_3), 0.82 (d, 6H; $\text{C}(\text{CH}_3)_2$).

$^{13}\text{C-NMR}$ (400 MHz, DMSO-d_6) δ (ppm): 179.22, 167.84, 167.57, 131.41, 131.23, 131.10, 41.60, 39.30, 36.45, 35.69, 32.56, 29.13, 27.73, 27.68, 24.73.

MS (MALDI-TOF, negative mode): m/z 492.23 (calculated); 492.27 (experimental).

FT-IR (powder) wavenumber (cm^{-1}): 1704 (m), 1695 (m), 1658 (s), 1338 (s), 1244 (s), 768 (s)

3.2.3 Synthesis of acid chloride **4**

Compound **3** (1eq, 70.6 mg, 0.14 mmol) was added in a two-neck 50 mL round bottom flask under Argon atmosphere. Dry dichloromethane (10 mL) was added and mixture was cooled with ice bath. Few drops of DMF and 60 μ L of oxalyl chloride (5 eq) were added dropwise. The mixture was left stirring overnight at room temperature. The day after the solvent was removed under high vacuum and the acid chloride **3** was directly used under Argon in the next step.

3.2.4 Synthesis of amide appended NDI **5**

10 mL of dry NMP were added to the acid chloride **4** under Argon atmosphere. Then aniline (2.5 eq, 32 μ L) was added as nucleophile and as base. The mixture was stirred at 60 °C 24h.

The mixture was then cooled to room temperature and poured into acidic water (pH 2-4) under vigorous stirring. The water solution was then filtered and the solid washed with water and cold methanol. The crude was purified by chromatographic column (silica gel, eluent CHCl₃/MeOH 95/5, R_f = 0.7) to afford 13 mg of compound **5** as yellowish powder (yield 18%).

¹H-NMR (400 MHz, CDCl₃) δ (ppm): 8.73 (dd, 4H; naphthalene), 7.75 (s, NH), 7.42 (d, CH; ortho), 7.2 (t, CH meta), 7.01 (t, CH para), 4.36-4.21 (m, 4H; NCH₂), 2.47 (t, 2H; CH₂CON), 2.25 (m, 2H; CH₂CH₂CON), 1.47 (m, 1H; NCH₂CH₂CH), 1.17-1.38 (m, 10H), 1.04 (d, 3H; CH₃), 0.85 (d, 6H; C(CH₃)₂).

¹³C-NMR (400 MHz, CDCl₃) δ (ppm): 170.22, 163.36, 162.64, 137.94, 131.13, 130.83, 128.79, 126.79, 126.6, 123.96, 119.33, 40.09, 39.42, 39.22, 37.06, 35.00, 31.23, 27.92, 24.60, 23.91, 22.68, 22.60, 19.53.

MS (MALDI-TOF, negative mode): m/z 567.27 (calculated); 567.30 (experimental).

FT-IR (powder) wavenumber (cm⁻¹): 3300 (bw), 1705 (m), 1668 (s), 1340 (m), 1252 (m), 769 (s).

Acknowledgements

This thesis is not just a work, but it is the result of a new experience. Like many new experience, it is not easy in the beginning but it could be useful and gratifying if you know how to take it on. Many many people helped me in this dutch adventure that I would like to thank.

Firstly, Prof. Meijer who gave me the chance to work six months in his group. It was a highly stimulating experience who made me grow up as scientist and person.

Secondly, my tutor Andreas who taught me a lot, answered all my questions, encouraged me when I was demoralized (several times), instead of just kick my head. I would like to thank the people in the best lab ever (lab 3 obviously) who made my days several times: Peter-Paul , Nic (great fume neighbours), Ghislaine, Janus, The Gosens Brothers, Ankush, BasdeWaal, Rob. All the people of the group, Andreas (the other one), Anja, Bram, Nora and many others for their support and their advices. I would also like to thank Bas for the synthesis of the chiral amine, Ralf for the Maldi analysis, Martin Lutz for the X-ray analysis. I am probably forgetting to thank many other people, but whoever met me during this experience taught me something anyway, and it is worth to remind it.

Ringraziamenti

Finalmente arriva la parte in italiano (che almeno qua, spero di non scrivere sgrammaticato).

Prima di tutto ringrazierei gli italiani dutchizzati, che rientrerebbero nei ringraziamenti di cui sopra. Dire grazie nella tua lingua però, è tutta un'altra cosa. Ringrazio José, il mio secondo tutor, che mi ha spiegato un sacco di cose, ha provato a insegnarmi l'arte degli NDI (e se siete arrivati a leggere fin qui avrete capito che è piuttosto importante), sempre in maniera tranquilla e rilassata. Bea, la mia tutor in terza direi, oltre che amica (sì, ho avuto bisogno di svariati tutor..), che ha fatto tutto il possibile e anche l'impossibile per aiutarmi e farmi sentire sempre un po' più a casa. In questi ardui compiti, anche Sabrina, Vito e Darione, sono stati pilastri fondamentali per la mia sopravvivenza e il mio benessere psicologico, sono persone fantastiche e spero di rivederli presto, magari al DeBurger, perché no. Grazie anche a Matteo e Federica, giovani espatriati come me con cui ho condiviso tanti pensieri sulla vita 'li fuori'.

Anche in Italia ho tante persone da ringraziare. Innanzitutto Francesco, che mi ha su(o)pportato sia a Pisa che a km di distanza, mi ha fatto compagnia e perché senza di lui avrei fatto e capito ben poco, da più di un anno ormai. Ringrazio inoltre il prof. Pescitelli per i consigli sulle caratterizzazioni chiroottiche. Vorrei ringraziare inoltre tutti i miei compagni di corso con cui ho condiviso gioie e dolori dell'organica, tra cui Margherita per i fantastici appunti, Luigi e MariaLuisa mitici compagni del gruppo di lab, Gabriele, Giovanni, Alberto per le sessioni di studio, e tutti gli altri colleghi che anche se non se ne accorgono forse, hanno fatto tanto. Un grazie speciale alle Nespole, con cui ho

condiviso tutta la mia vita da studente universitario e che sono una seconda famiglia a Pisa. Grazie ai musicanti con cui ho passato sonore ore liete, al gruppo di Impro, ai miei coinquilini vecchi e nuovi. A Giuseppe e Guido per le piacevoli chiacchierate, a Miki per avermi insegnato l'arte dello zen, a Rob e Gigi per le consulenze informatiche senza le quali questa tesi sarebbe stata scritta con la biro probabilmente. Le persone da ringraziare sono queste e sicuramente tante altre. Grazie a Simona, la mia fan numero uno, a mia sorella e ai miei genitori che credono sempre in me.